DOCTORAL SCHOOL
MEDITERRANEA UNIVERSITY OF REGGIO CALABRIA

DEPARTMENT OF INFORMATION ENGINEERING, INFRASTRUCTURES
AND SUSTAINABLE ENERGY
(DIIES)

PHD IN
INFORMATION ENGINEERING

S.S.D. ING-INF/02
XXVIII CYCLE

TARGET TRACKING IN MARINE ENVIRONMENT FROM X-BAND RADAR DATA

CANDIDATE
Daniele ARTURI

ADVISOR
Dr. Lorenzo CROCCO

CO-ADVISOR
Ing. Francesca SERAFINO

COORDINATOR
Prof. Claudio DE CAPUA

REGGIO CALABRIA, FEBRUARY 2016

Finito di stampare nel mese di **Febbraio 2016**

Edizione 

Collana *Quaderni del Dottorato di Ricerca in Ingegneria dell'Informazione*
Curatore *Prof. Claudio De Capua*

ISBN 978-88-99352-02-8

Università degli Studi *Mediterranea* di Reggio Calabria
Salita Melissari, Feo di Vito, Reggio Calabria

DANIELE ARTURI

TARGET TRACKING IN MARINE ENVIRONMENT FROM X-BAND RADAR DATA

The Teaching Staff of the PhD course in
INFORMATION ENGINEERING
consists of:

Claudio DE CAPUA (coordinator)
Raffaele ALBANESE
Giovanni ANGIULLI
Giuseppe ARANITI
Francesco BUCCAFURRI
Giacomo CAPIZZI
Rosario CARBONE
Riccardo CAROTENUTO
Salvatore COCO
Mariantonia COTRONEI
Lorenzo CROCCO
Francesco DELLA CORTE
Lubomir DOBOS
Fabio FILIANOTI
Domenico GATTUSO
Sofia GIUFFRE'
Giovanna IDONE
Antonio IERA
Tommaso ISERNIA
Fabio LA FORESTA
Gianluca LAX
Aime' LAY EKUAKILLE
Giovanni LEONE
Massimiliano MATTEI
Antonella MOLINARO
Andrea MORABITO
Carlo MORABITO
Giuseppe MUSOLINO
Roberta NIPOTI
Fortunato PEZZIMENTI
Nadia POSTORINO
Ivo RENDINA
Francesco RICCIARDELLI
Domenico ROSACI
Giuseppe RUGGERI
Francesco RUSSO
Giuseppe SARNE'
Valerio SCORDAMAGLIA
Domenico URSINO
Mario VERSACI
Antonino VITETTA

To my father

Contents

CONTENTS ..... **VII**

LIST OF FIGURES ..... **IX**

LIST OF TABLES ..... **XIII**

1 INTRODUCTION **1**

1.1 INTRODUCTION ON RADAR PRINCIPLES 4
1.2 RADAR PROPERTIES 5
1.3 TARGET TRACKING AS AN ESTIMATION PROBLEM 7
1.4 THE ASSOCIATION PROBLEM AND THE VALIDATION REGION 10
1.5 AIM AND OUTLINE OF THE THESIS 12

2 TRACKING ISSUES AND OVERVIEW OF THE PRINCIPAL ALGORITHMS **15**

2.1 TRACK A SINGLE TARGET IN CLUTTER 15
2.2 TRACK MULTIPLE TARGETS IN CLUTTER 17
2.3 INTRODUCTION TO TRACKING ALGORITHMS 18
2.4 KALMAN FILTER 19
2.4.1 NEAREST NEIGHBOR STANDARD KALMAN FILTER (NNSKF) 22
2.4.2 STRONGEST NEIGHBOR STANDARD KALMAN FILTER (SNSKF) 23
2.5 PROBABILISTIC DATA ASSOCIATION (PDA) 23
2.5.1 JOINT PROBABILISTIC DATA ASSOCIATION FILTER (JPDAF) 27
2.5.1.1 CHEAP PDAF AND CHEAP JPDAF 28
2.6 MULTIPLE HYPOTHESIS TRACKING (MHT) 29
2.7 INTERACTIVE MULTIPLE MODEL (IMM) 31

3 VALIDATION OF TRACKING ALGORITHMS ON SIMULATED DATA **33**

3.1 DATA CHARACTERISTICS 33
3.2 THE CLUTTER MODEL 34
3.3 MODEL FOR FALSE DETECTION 36
3.4 SINGLE TARGET TRACKING 38
3.5 MULTI TARGET TRACKING 47
3.6 RESULTS AND OBSERVATIONS 55

4 X BAND RADAR TARGET TRACKING IN MARINE ENVIRONMENT: A COMPARISON OF DIFFERENT ALGORITHMS IN A REAL SCENARIO **57**

4.1 INTRODUCTION TO X-BAND RADAR 57
4.2 VALIDATION OF TRACKING ALGORITHMS ON REAL DATA ACQUIRED BY AN X-BAND RADAR 58
4.3 CLUSTERING 60
4.4 K-DISTRIBUTED CLUTTER 61
4.5 RESULTS AND OBSERVATIONS 64

5 CONCLUSIONS AND FUTURE PERSPECTIVES **73**

REFERENCES **75**

PUBLICATIONS **81**

List of Figures

Fig. 1.1 Basic principle of radar 4
Fig. 1.2 Mathematical view of state estimation 7
Fig. 1.3 Block diagram of target state estimation 8
Fig. 1.4 Optimal estimator issues 9
Fig. 1.5 Validation gate 10
Fig. 2.1 Single target in clutter 15
Fig. 2.2 Multiple targets in clutter 17
Fig. 2.3 Main tracking algorithms 18
Fig. 2.4 State estimation system (part 1) 20
Fig. 2.5 State estimation system (part 2) 21
Fig. 2.6 Kalman filter feedback control 22
Fig. 2.7 NNSKF Functionality 22
Fig. 2.8 PDAF Functionality 24
Fig. 2.9 Typical MTT system 29
Fig. 2.10 Association ambiguity 30
Fig. 2.11 General functionality of IMM 31
Fig. 3.1 Sea clutter origin (v, wind direction) 35
Fig. 3.2 Binomial distribution of false alarms 36
Fig. 3.3 False alarms distribution in function of their spatial density 37
Fig. 3.4a Single target without clutter (acquisition time t1) 38
Fig. 3.5b Single target without clutter (acquisition time t2) 39
Fig. 3.6c Single target without clutter (acquisition time t3) 39
Fig. 3.7a Single target with clutter assuming 3 false alarms every time instant tracked with NNSKF (acquisition time t1) 41
Fig. 3.8b Single target with clutter assuming 3 false alarms every time instant tracked with NNSKF (acquisition time t2) 41
Fig. 3.9c Single target with clutter assuming 3 false alarms every time instant tracked with NNSKF (acquisition time t3) 42
Fig. 3.10a Single target with clutter assuming 10 false alarms every time instant tracked with NNSKF (acquisition time t1) 42
Fig. 3.11b Single target with clutter assuming 10 false alarms every time instant tracked with NNSKF (acquisition time t2) 43
Fig. 3.12c Single target with clutter assuming 10 false alarms every time instant tracked with NNSKF (acquisition time t3) 43
Fig. 3.13a Single target with clutter assuming 3 false alarms every time instant tracked with Cheap PDAF (acquisition time t1) 44
Fig. 3.14b Single target with clutter assuming 3 false alarms every time instant tracked with Cheap PDAF (acquisition time t2) 45
Fig. 3.15c Single target with clutter assuming 3 false alarms every time instant tracked with Cheap PDAF (acquisition time t3) 45
Fig. 3.16a Single target with clutter assuming 10 false alarms every time instant tracked with Cheap PDAF (acquisition time t1) 46
Fig. 3.17b Single target with clutter assuming 10 false alarms every time instant tracked with Cheap PDAF (acquisition time t2) 46

Fig. 3.18c Single target with clutter assuming 10 false alarms every time instant tracked with Cheap PDAF (acquisition time t3) 47
Fig. 3.19a Two targets with clutter assuming 3 false alarms every time instant tracked with NNSKF (acquisition time t1) 48
Fig. 3.20b Two targets with clutter assuming 3 false alarms every time instant tracked with NNSKF (acquisition time t2) 48
Fig. 3.21c Two targets with clutter assuming 3 false alarms every time instant tracked with NNSKF (acquisition time t3) 49
Fig. 3.22a Two targets with clutter assuming 10 false alarms every time instant tracked with NNSKF (acquisition time t1) 50
Fig. 3.23b Two targets with clutter assuming 10 false alarms every time instant tracked with NNSKF (acquisition time t2) 50
Fig. 3.24c Two targets with clutter assuming 10 false alarms every time instant tracked with NNSKF (acquisition time t3) 51
Fig. 3.25a Two targets with clutter assuming 3 false alarms every time instant tracked with Cheap JPDAF (acquisition time t1) 51
Fig. 3.26b Two targets with clutter assuming 3 false alarms every time instant tracked with Cheap JPDAF (acquisition time t2) 52
Fig. 3.27c Two targets with clutter assuming 3 false alarms every time instant tracked with Cheap JPDAF (acquisition time t3) 52
Fig. 3.28a Two targets with clutter assuming 10 false alarms every time instant tracked with Cheap JPDAF (acquisition time t1) 53
Fig. 3.29b Two targets with clutter assuming 10 false alarms every time instant tracked with Cheap JPDAF (acquisition time t2) 54
Fig. 3.30c Two targets with clutter assuming 10 false alarms every time instant tracked with Cheap JPDAF (acquisition time t3) 54
Fig. 4.1 Architecture of the acquisition and processing system of the radar data 58
Fig. 4.2 Installation site of the Remocean system indicated by the red circle 59
Fig. 4.3 Radar image showing clutter and moving targets at the port of Giglio Island 60
Fig. 4.4 Radar image with three targets indicated by the red circles 60
Fig. 4.5 Block diagram of a detection and tracking system 61
Fig. 4.6 Pdf of the K-distribution for $\boldsymbol{b}$ =1 and $\boldsymbol{\nu = 0.5}$ (blue), $\boldsymbol{\nu = 1}$ (violet) and $\boldsymbol{\nu = 5}$ (yellow) 64
Fig. 4.7a Real data acquired by the X-band radar system tracked with NNSKF (acquisition time t1) 65
Fig. 4.7b Real data acquired by the X-band radar system tracked with NNSKF (acquisition time t2) 65
Fig. 4.7c Real data acquired by the X-band radar system tracked with NNSKF (acquisition time t3) 66
Fig. 4.7d Real data acquired by the X-band radar system tracked with NNSKF (acquisition time t4) 66
Fig. 4.8a Real data acquired by the X-band radar system tracked with Cheap PDAF (acquisition time t1) 67
Fig. 4.8b Real data acquired by the X-band radar system tracked with Cheap PDAF (acquisition time t2) 67
Fig. 4.8c Real data acquired by the X-band radar system tracked with Cheap PDAF (acquisition time t3) 68

Fig. 4.8d Real data acquired by the X-band radar system tracked with Cheap PDAF (acquisition time t4) 68
Fig. 4.9a Real data acquired by the X-band radar system tracked with Cheap JPDAF (acquisition time t1) 69
Fig. 4.9b Real data acquired by the X-band radar system tracked with Cheap JPDAF (acquisition time t2) 69
Fig. 4.9c Real data acquired by the X-band radar system tracked with Cheap JPDAF (acquisition time t3) 70
Fig. 4.9d Real data acquired by the X-band radar system tracked with Cheap JPDAF (acquisition time t4) 70

List of Tables

Tab. 1.1 Frequency band in the range of microwaves..... 5
Tab. 3.1 Main parameters..... 33
Tab. 4.1 Parameters of the acquisition system..... 57
Tab. 4.2 Parameters of the elaboration system..... 64

1

Introduction

Radar surveillance applications are essentially based on target detection and tracking techniques, which are classic radar problems [1]. The aim is to provide the coordinates, the speed, the course and the behavior of a moving target or, in other words, to "follow" a target that moves along the sea surface. To this end, in the initial stage, the radar must detect the presence of the target within the scene under observation, through the so-called identification or detection procedure. Then, the tracking procedure is based on the analysis of a set of detection measures, associated with the same target, carried out at different time instants. Therefore, tracking is closely related to detection, so that a proper tracking must take into account all the problems connected with detection [2].

In a given instant of time, the radar provides a set of measures that may come from the target of interest, may be due to false alarms or clutter, or may have been generated from other targets. After the detection procedure, only the measures that come from the target of interest in the following time instants are considered, thus, defining the tracking of that target, namely the set of its positions in time. Consequently, given the set of all positions of a target up to the current time, it is possible to "predict" the position in the next measurement associated with that target [3].

During the tracking procedure, measurements that come from a target are processed in order to obtain an estimate of its current state [4], which typically consist of:

- Kinematic components — position, velocity, acceleration, turn rate, etc.
- Feature components — radiated signal strength, spectral characteristics, radar cross-section, target classification, etc.

Target detection strategies aim to distinguish the radar echo of the electromagnetic return of a target from the unwanted signal (noise), which can affect the detection performances [5]. Obviously, in a multi-target scenario, it is more difficult to establish that the measurement received by the radar is originated from a particular target and, in addition to this, the output of a detection algorithm is characterized by the presence of false alarms, which can be interpreted as measurement noise and further complicate the target state estimate [6].

In marine environment, target tracking has a specific methodological interest, because it requires dealing with the peculiar problems related to the separation of useful signal from clutter signal, which can induce false alarms and ultimately lead to the loss of the target [7]. These issues, of course, call for proper solution procedures to address the classic problems of target tracking, namely the correct detection of targets and the association procedure, needed to determine which one of the detected signals has been originated by the target of interest [8]-[12].
The primary objective of target tracking is to estimate the state trajectories of a target. In the case of target moving on the sea surface, the main problems are:

- clutter, due to the presence of the capillary waves generated by the wind;
- target model uncertainties, due to the unexpected maneuver of the ship;
- measurement uncertainties, due to the presence of environmental and instrumental noise

X-band radar systems are used in a great variety of civil and military problems applications, weather monitoring and vessel traffic control. As regards applications in marine environment, they are considered a flexible and low-cost tool for ship detection and have attracted a growing interest in last decade, thanks to their capability of scanning the sea surface with high

temporal and spatial resolution, their cost-effectiveness, as well as their simplicity of operation and installation [13]. However, in spite of their versatility, incoherent X-band radars are mostly employed for high resolution surveillance purposes but, in these scenarios, they cannot be considered as reliable as coherent systems in terms of target detection capabilities, with a consequent limitation in terms of target tracking. This is due to the fact that the result of a processing based only on the amplitude of the received signal that can be compromised by the presence of sea clutter, conversely coherent systems, by measuring both the amplitude of the signal received and its phase, can be more accurate. However, the employment of an effective tracking strategy can play a fundamental role in these circumstances, leading to a significant improvement in the surveillance performances provided by such coherent radar systems.

The thesis is organized as follows. Chapter 1 provides a study of the problematic of the identification and tracking of a moving target and the association procedure. Chapter 2 deals with some tracking problems and offers an overview of the principal tracking algorithms. Chapter 3 presents the validation and implementation of some of these algorithms on simulated data, including a description of the false alarm distribution. Chapter 4 presents the validation and implementation of some of these algorithms on real data acquired by an X-band radar installed at the port of the Giglio island, including a description of the clutter distribution. Chapter 5 presents the conclusions and the future perspectives.

1.1 Introduction on RADAR principles

The term RADAR indicates an electronic apparatus used to detect the presence and measure of the position of objects (targets) by means of radio waves. This measure consists in determining the distance and the direction of objects from the radar, analyzing the signal backscattered by the target [14].
The operation of a radar is very simple: the same antenna transmits a signal and receives the echo due to reflections on possible obstacles, i.e., the targets. The distance is determined by measuring the time interval that elapses between the transmission and reception of the pulses, being known the speed of propagation of radio waves:

$$R = \frac{c\Delta t}{2} \tag{1.1}$$

(it must be considered the time of go and return of the signal).

If the transmitted pulses do not encounter any obstacle during their propagation, then they do not return back, that is, the signal travels unperturbed and it will be attenuated as the distance increases, while, in the case in which the beam hits an object, the signal is reflected and an echo is revealed from the receiver antenna [15] (Fig. 1.1).

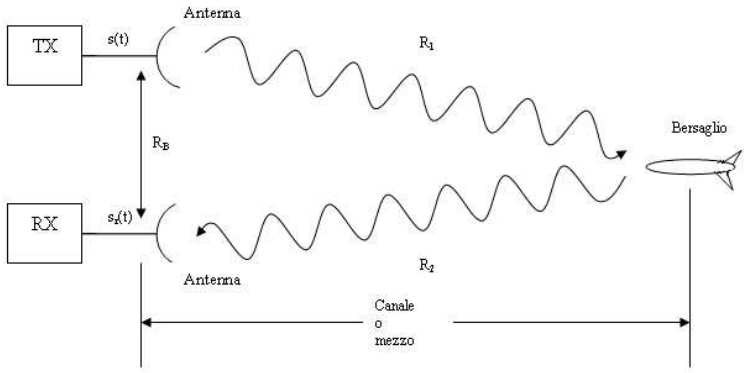

Fig. 1.1 Basic principle of radar

The type of electromagnetic radiations emitted by radar antennas are located within the microwave range. Following World War II, there is a classification of the electromagnetic radiation type according to different regions of wavelength:

Band	Frequency (Ghz)	Wavelength (cm)
P	0.225 - 0.39	77 - 133
L	0.39 – 1.55	19 - 77
S	1.55 – 3.90	7.7 – 19
C	3.90 – 6.20	4.8 – 7.7
X	5.75 – 10.9	2.8 – 5.2
Ku	10.9 – 18.0	1.7 – 2.8
Ka	18.0 – 36.0	0.8 – 1.7

Tab. 1.1 Frequency band in the range of microwaves

1.2 Radar properties

The operation of the radar is characterized by the following properties [16]:

Sensitivity refers to the ability of the radar to detect the reflected signal also from weak targets. Normally, it is taken as the minimum input signal required to produce a specified output signal and it represents a measure of the interference generated by the radar (self-noise) against the minimum signal it is able to detect.

The **measurements** of the distance from the target is inherent in the name radar. The modern radar systems are capable of measuring the position of the target in a three dimensional space, its velocity vector and the angular direction of the vector of the angular speed and all these measurements may be made on more targets of interest with the presence of clutter and noise. The most advanced radar have also the ability to measure the extent, the shape and the classification of the target (person, building, airplane, etc.).

The **resolution** corresponds to the ability of the radar to locate the desired target and distinguish it from the noise and clutter. In practice, there is a limitation in the resolution achievable due to the characteristics of the signal and the antenna. In particular, as regards the limitation in the resolution, it can be observed that a greater bandwidth provides better resolution in range, while a longer pulse durations allow improving frequency resolution.

Radar resolution is formally expressed by two figures: resolution in range and resolution in azimuth.

1. Resolution in range is the minimum distance that must exist between two objects such that the system is able to discriminate them, otherwise they become indistinguishable. It is defined as

$$\Delta r_{\min} = \frac{c\tau}{2} \quad , \qquad (1.2)$$

where c is the speed of light and τ it is the pulse duration.

2. Resolution in azimuth is the ability of radar equipment to separate two reflectors at similar ranges but different bearings from a reference point. It is defined as

$$\Delta\Phi \approx \frac{\lambda}{D} \qquad (1.3)$$

The expression is valid for large distances, where λ is the wavelength of the signal and D is the effective diameter of the antenna.

1.3 Target tracking as an estimation problem

Estimation is the process of inferring the value of a quantity of interest from indirect, inaccurate and uncertain observations [17]. The variable of interest in an estimation problem can be:

- a parameter — a time-invariant quantity (a scalar, a vector or a matrix);
- the state of a dynamic system (usually a vector).

In this context, tracking procedures can be viewed as the estimation of the state of a moving object.

The block diagram in Fig. 1.2 represents a general conceptual representation of the state estimation problem.

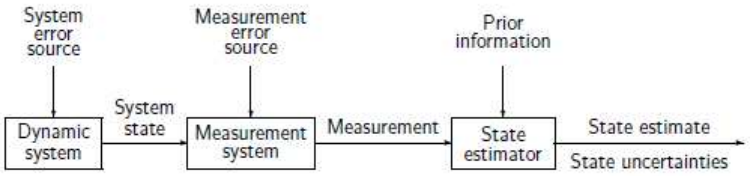

Fig. 1.2 Mathematical view of state estimation

There is no possibility to access to variables inside the dynamic and measurement systems, therefore the only variables which are available to the estimator are the measurements, which are obviously affected by the error sources modeled in the form of "noise."

An optimal estimator is a computational algorithm that processes observations (measurements) to yield an estimate of a variable of interest, that minimizes a certain error criterion.

As a consequence:

- the advantage of an optimal estimator is that it exploits the data and the knowledge of the system and of the noise in the best possible way (through a proper model);

- the disadvantages are that it is sensitive to modeling errors and might be computationally expensive.

The block diagram in Fig. 1.3 is an extended version of the one in Fig. 1.2, which explains more in detail the conceptual representation of the dynamic system where detection and tracking are operating, the measurement system used to acquire data and the state estimator used to produce the results.

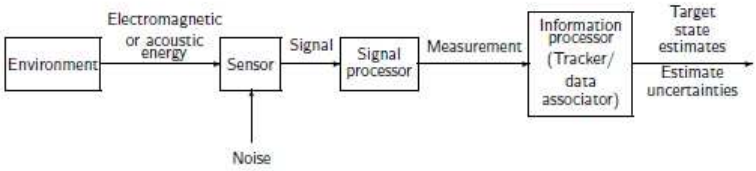

Fig. 1.3 Block diagram of target state estimation

The correspondences with the block diagram in Fig. 1.2 are the following:

- the block "Environment" refers to the block "Dynamic system";
- the blocks "Sensor" and "Signal Processor" refer to the block "Measurement system";
- the block "Information Processor" refers to the block "State estimator".

Active sensors, like radars, emit energy into the environment and search for reflected energy. The backscattered signal is then processed by the signal processor and there is a measure. The measurements of interest are not raw data points but usually the outputs of complex signal processing and detection subsystems. Finally, the measurement is processed in order to obtain the target state estimate.

However, many problems can arise in a target detection and tracking procedure, as illustrated in Fig. 1.4. These problems can seriously affect the detection and tracking procedure and eventually compromise the outcome of the target state estimate.

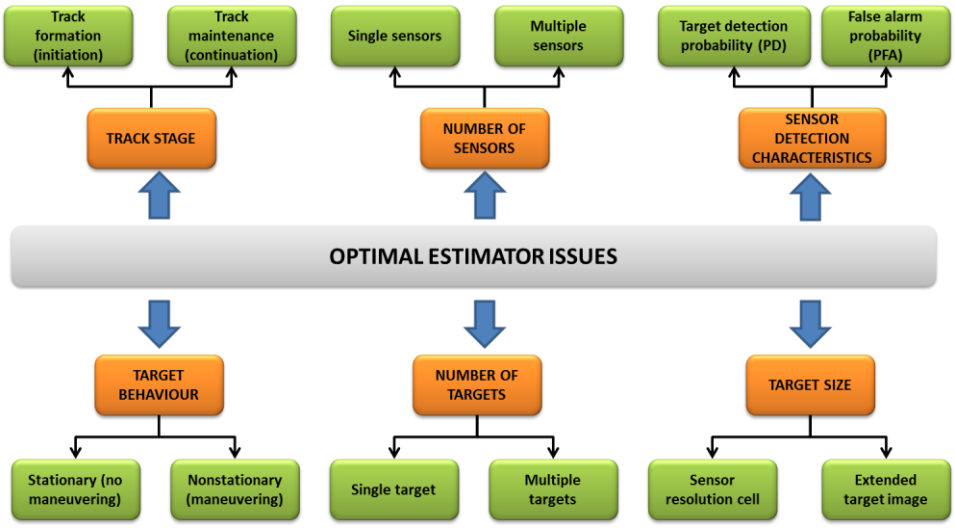

Fig. 1.4 Optimal estimator issues

As shown in the central part of the figure, the first two problems to take into account are:

- *the number of sensors* used to perform the tracking procedure, since a single-sensor or a multi-sensor tracking procedure can be performed, considering that adding additional sensors to the observation system can produce a more accurate estimate of the trajectory, even though the multi-sensor tracking is subject to other issues to face;
- *the number of targets* to be tracked, which is a not well defined number. Obviously, it is more difficult to track more targets all together and at the same time, because, if the system parameters are not properly defined, the signal of a target can produce interference to the signal of another target.

The right side of the figure shows the following problems:

- *track stage*, in particular the track formation (or initiation), it means when the target is "seen" for the first time, and the track maintenance (or continuation), that is the ability to continue to follow the same target, a complex operation due to the presence of the false alarms because they can affect the tracking procedure;

- if the *target behavior* is stationary or no stationary, that is if the movement of the target is subject to maneuvering or not, because in the no stationary case the target can suddenly change its trajectory possibly compromising its estimate.

Finally, the right side of the figure shows the problems of defining the:

- *Sensor detection characteristics*, that is Probability of Detection (PD) and Probability of False Alarms (PFA), which are parameters used during the detection and tracking procedure that must be carefully evaluated in order to obtain a correct target trajectory estimate;
- *Target size*, that is if the dimension of the target is comparable to the sensor resolution cell or if the target image is an extended one; the second case is more complex to deal with because the target signal received by the system is actually composed of a cloud of points.

1.4 The association problem and the validation region

Let us suppose that the set of all the positions occupied by the target up to the current time k-1 is known. Then, one can "predict" the position where it is more probable to find the next measurement associated with that target at instant k. The new measures provided by the radar will be, presumably, in a validation or association region (gate) located around the predicted value [9], [10]. The size of this region depends on many factors, including the measurement errors, the uncertainty on the position of the target and the uncertainty about its motion.

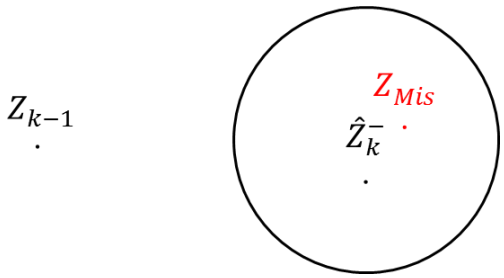

Fig. 1.5 Validation gate

However, for a fixed time instant, the radar provides a series of measures which may:

- come from the target of interest;
- be due to false alarms or clutter;
- have been generated from other targets.

In that case, uncertainty in data association arises because it is not possible to know a priori, for each measure, the source from which the recorded signal has been generated. This uncertainty occurs when the signal from the target is weak. In order to detect it, the detection threshold has to be lowered, which has the obvious drawback that background signals and sensor noise may also be detected, yielding clutter or spurious measurements. This situation can also occur when several targets are present in the same neighborhood [21]. Introducing spurious measurements in a tracking filter leads to divergence of the estimation error and, thus, track loss.
This uncertainty, if not resolved in the most appropriate manner, can lead to the loss of the target.
A measure that is within the region of association becomes "candidate" to the association, although it is not guaranteed that it has been originated from the target of interest. This procedure prevents the measure relative to the target of interest to be searched in the entire observation scenario and limits to search measures only internal to the gate. Consequently, the measures in areas outside of the gate can be ignored because they are too distant from the predicted measure and it is not likely that they have been originated from the target of interest.

Let us suppose to track a single target, the following cases can arise:

1. one of the measures will be associated with the target of interest, while the others will be associated with clutter or other targets;
2. all the measures are exclusively associated with clutter;
3. there are no measures.

Consequently:

- the first problem is to select measurements to be used to update the state of the target of interest in the tracking filter;
- the second problem is to determine whether the filter has to be modified to account for this data association uncertainty.

The goal is to obtain the minimum mean square error (MMSE) estimate of the target state and the associated uncertainty [18].

1.5 Aim and outline of the thesis

This thesis is concerned with the implementation and validation of algorithms for tracking targets moving on the sea surface.

From a methodological point of view, the thesis is divided into two parts.

The first part is a study of the issues arising in identification and tracking of a moving marine target and of the association procedures used to determine whether the measure received by the radar is correctly referred to the target (a ship) from which it was generated.

The second part of the thesis deals with the problem of sea clutter that may corrupt or even compromise the state estimate of the target, because, if clutter is strong enough, it becomes difficult to distinguish the useful component of the signal arising from the target, with obvious consequences on the association phase. This problem required a proper tuning of the parameters of the algorithms based on the statistics of the clutter of reference.

In particular, two variants of the main target tracking algorithm present in the literature [19], the Kalman Filter (KF), have been analyzed: the Nearest Neighbor Standard Kalman Filter (NNSKF) and Strongest Neighbor Standard Kalman Filter (SNSKF) have been considered and validated (on simulated data).

Since these algorithms have evidenced a significant occurrence of false alarms, the attention has been then focused on the Probabilistic Data Association Filter (PDAF) for the single tracking and for multi tracking

version the Joint-PDAF (JPDAF) [20], [21]. Also the "cheap" variants of these algorithms have been considered and validated on real data.

As a significant case study used to validate the developed procedures and algorithms, we have exploited the data collected by an X-band radar installed at the port of the Giglio island. On 13th of January 2012, Costa Concordia cruise ship, with about 4200 passengers onboard, smashed against the coast of Giglio Island, located in the Tuscan Archipelago, in the Northwestern Mediterranean Sea.

To face such a kind of disaster, the state of emergency was declared and a number of different devices were installed on the island to monitor the ship wreck, to prevent oil spills in the sea or the definitive sinking of the wreck because of the coastal storms. The Remocean system was one of these systems and it was purchased by the Tuscany Region, installed at the Giglio Island and managed by the LaMMA Consortium as a supporting observational tool providing information about the sea state, which was important for the removal operations of the Costa Concordia ship wreck.

The use of real data gave us the opportunity to address two main issues:

1. the first one, very thorny, is the sea clutter, therefore validating the tracking algorithms also in conditions in which the useful signal backscattered to the radar is not perfectly clean, but it is compromised by the presence of the sea, in particular, by the capillary waves generated by the wind;
2. the second, as will be explained further on, has allowed to understand how the targets are no longer point type, but they are represented by a cloud of points, so they must be considered with an extended shape with their suitable dimensions, further complicating the whole processing system.

2

Tracking issues and overview of the principal algorithms

2.1 Track a single target in clutter

The problem of tracking a single target in clutter considers the situation where there are possibly several measurements in the validation region (gate) of a target. The set of validated measurements consists of:

- the correct measurement (if detected and it falls in the validation gate);
- the undesirable measurements (originated by clutter or false-alarm).

The common mathematical model for such false measurements is that they are uniformly spatially distributed and independent across time.

The validation procedure limits the region in the measurement space where it is more probable to find the measurement from the target of interest. In addition, it can happen that several measurements will be found in the validation region and that those falling outside the validation region can be ignored because they are "too far" from the predicted state and thus very unlikely to have originated from the target of interest. This holds true if the gate probability is close to unity and the model used to obtain the gate is correct [1], [4], [9]. A situation with several validated measurements is depicted in Figure 2.1.

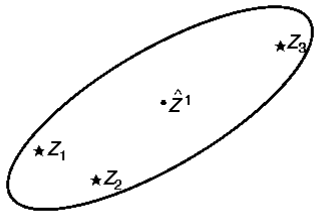

Fig. 2.1 Single target in clutter

The two-dimensional validation region in Figure 2.1 is an ellipse centered at the predicted measurement $\widehat{Z^1}$. The elliptical shape of the validation region is defined by [1], [4], [9]

$$V(k,\gamma) = \{z: [z_k - \hat{z}_k^-]^T S^{-1} [z_k - \hat{z}_k^-] \leq \gamma\} \quad (2.1)$$

where

- $[z_k - \hat{z}_k^-]$ is the innovation term given from the difference between the real measure and the respective estimate
- S is the covariance of the innovation
- γ is the gate threshold
- k is the instant of time

The error in the target's predicted measurement, that is, the innovation, typically follows a Gaussian distribution and the parameters of this ellipse are determined by the covariance matrix S of the innovation. All the measurements in the validation region may have been originated from the target of interest, but only one of them is the true one.
As a consequence, the set of possible association events are the following:

a) Z_1originated from the target, and Z_2 and $Z_3$are spurious;
b) Z_2originated from the target, and $Z_1$and $Z_3$are spurious;
c) Z_3originated from the target, and $Z_1$and $Z_2$are spurious;
d) all measurements are spurious.

These association events are mutually exclusive and exhaustive so it is possible to use the total probability theorem in order to obtain the state estimate in the presence of data association uncertainty. Under the assumption that there is a single target, the spurious measurements constitute a random interference.

2.2 Track multiple targets in clutter

When several targets as well as clutter or false alarms are present in the same neighborhood, the data association becomes more complicated [9], [21]. Figure 2.2 illustrates this case, where the predicted measurements for the two targets are denoted as $\widehat{Z^1}$and $\widehat{Z^2}$:

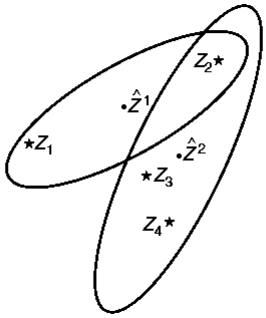

Fig. 2.2 Multiple targets in clutter

Three association events are possible:

a) Z_1 is originated from target $\widehat{Z^1}$ or clutter;

b) Z_2 is originated from either target $\widehat{Z^1}$ or target $\widehat{Z^2}$ or clutter;

c) Z_4 and Z_5 are originated from target $\widehat{Z^2}$ or clutter.

However, if Z_2 is originated from target $\widehat{Z^2}$ then it is likely that Z_1 is originated from target $\widehat{Z^1}$ In this situation, a persistent interference from a neighboring target is present in addition to random interference or clutter, therefore joint association events must be considered. Consequently, in view of the fact that any signal processing system has an inherent finite resolution capability, the additional possibility that Z_2 could be the result of the merging of the detections from the two targets has to be considered: this measurement is an unresolved one. The unresolved measurement constitutes another origin hypothesis for a measurement that lies in the intersection of two validation regions and this illustrates the difficulty of associating measurements to tracks [1], [4], [9].

2.3 Introduction to tracking algorithms

Two different approaches are considered in associating the data [1], [5], [9], [10]:

- Non-Bayesian data association — in this approach a decision procedure is established, using statistical tools, but, after the association decision, it is (possibly wrongly) assumed that the association is always correct.
- Bayesian (Probabilistic) data association — in this approach probabilities of associations are evaluated and used throughout the whole estimation process.

Both of these approaches rely on certain models of the targets and the sensors from which the measurements are obtained. Significant difficulties are encountered in the modeling of the behavior of the targets, because they can maneuver, so they can present different behavior modes. This compounds the already complex problem of associating measurements under uncertainty. Figure 2.3 summarizes the principal tracking algorithms.

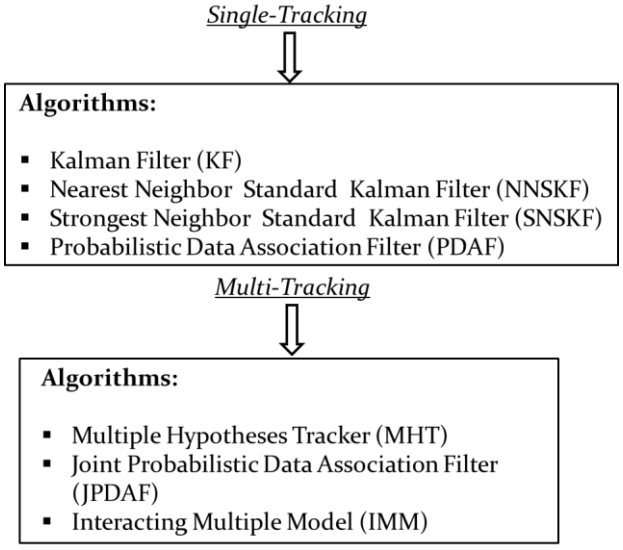

Fig. 2.3 Main tracking algorithms

2.4 Kalman Filter

Filtering is desirable in many situations in engineering because a good filtering algorithm can remove the noise from signals while retaining the useful information. Kalman filter estimates the states of a linear system and, among all possible filters, it is the one that minimizes the variance of the estimation error.

In order to control the position of a ship, a reliable estimate of the present position of the ship is needed and, to use a Kalman filter to remove noise from a signal, the process that is going to be measured has to be reliably described by a linear system.

A linear system is simply a process that can be described by the following two equations [4], [9]-[11]:

$$s_{k+1} = A_k s_k + B_k u_k + w_k \tag{2.2}$$

$$z_k = C_k s_k + n_k \tag{2.3}$$

where

$$E(w_k w_j^T) = Q_k \delta_{k-1} \tag{2.4}$$

$$E(n_k n_j^T) = R_k \delta_{k-1} \tag{2.5}$$

$$E(w_k n_j^T) = 0 \tag{2.6}$$

In the above equations

- A, B, and C are state transition matrices;
- k is the time index;
- s is called the state of the system;
- u is a known input to the system;
- z is the measured output;
- w and n are, respectively, the process noise and the measurement noise.

Generally, these quantities are vectors and therefore contain more than one element. The vector s contains all the information about the present state of the system. However, s cannot be measured directly; instead, it is analyzed the measure z (which is a function of s), which is corrupted by the noise n. It is possible to use z to obtain an estimate of s, but the information taken from z is corrupted by noise.

This situation is depicted in Fig. 2.4, where

- ✓ the real system and the model are fed with the same input $u(t)$
- ✓ the «^» symbol, used in the model, denotes the state and the exit estimates

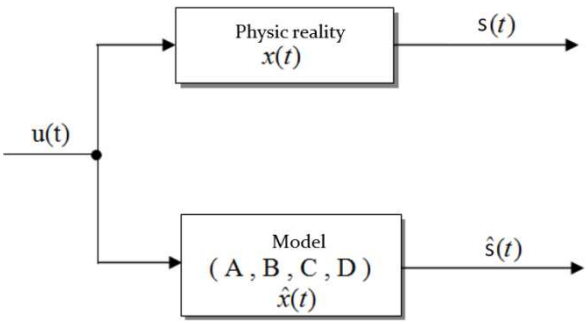

Fig. 2.4 State estimation system (part 1)

Let us now consider the difference between s(t) and $\hat{s}(t)$ as a parameter that indicates the accuracy of the estimate. The resulting error

$$e(t) = s(t) - \hat{s}(t) \qquad (2.7)$$

is commonly denoted as *innovation*.

In order to have a good estimate of $x(t)$ and, therefore, s(t), the prediction error $e(t)$ should be:

- Small
- Zero mean
- White

It is possible to use the error $e(t)$ to improve the state estimate, using the scheme depicted in Fig. 2.5

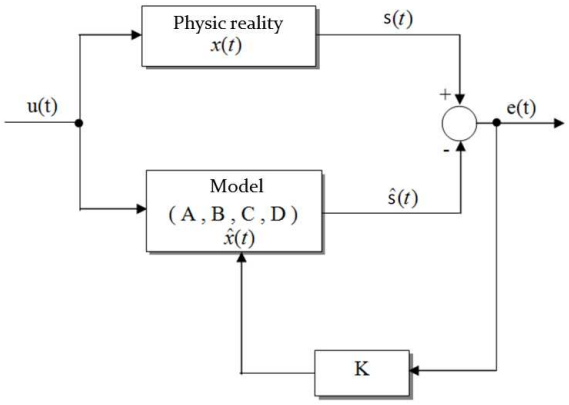

Fig. 2.5 State estimation system (part 2)

The gain K allows to weigh the error and return it within the model to correct the estimate of the state.
Let us consider the a priori and the a posteriori estimates:

$\widehat{s_k^-} = E[s_k|z_1, \dots, z_{k-1}]$ ⟶ A priori estimate

$\widehat{s_k^+} = E[s_k|z_1, \dots, z_k]$ ⟶ A posteriori estimate

where:

- $\widehat{s_k^-}$ indicates the state estimate obtained for the instant k, considering all the measurements until the k-1 instant (a priori);
- $\widehat{s_k^+}$ indicates the state estimate obtained for the instant k, considering all the measurements until the k instant (a posteriori).

The Kalman filter estimates a process by using a form of feedback control: the filter estimates the process state at some time and then obtains feedback in the form of (noisy) measurements, see Fig. 2.6.

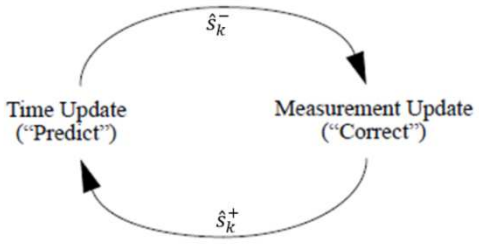

Fig. 2.6 Kalman filter feedback control

The time update equations are responsible for projecting forward (in time) the current state and error covariance estimates to obtain the a priori estimates for the next time step.

The measurement update equations are responsible for the feedback, for incorporating a new measurement into the a priori estimate to obtain an improved a posteriori estimate.

2.4.1 Nearest Neighbor Standard Kalman Filter (NNSKF)

In target tracking, the measurement that is "closest" to the predicted target-originated measurement is known as the nearest neighbor (NN) measurement, see Fig. 2.7.

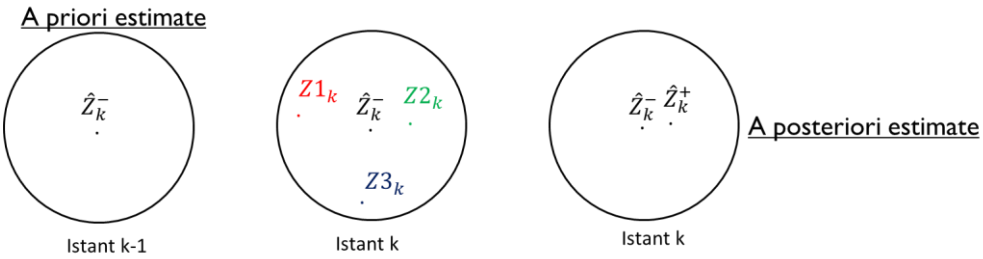

Fig. 2.7 NNSKF Functionality

A Kalman filter relying on this assumption is designated as *Standard* filter and considers that the assignment as correct, without accounting for the possibility that it might be erroneous [9], [16].

2.4.2 Strongest Neighbor Standard Kalman Filter (SNSKF)

When tracking targets in clutter, it is possible to have more than one measurement at any time, since a measurement may have originated from the target, clutter, false alarm or some other source.

In target tracking, the measurement that has the strongest intensity (amplitude) is known as the strongest neighbor (SN) measurement [9], [15].

2.5 Probabilistic Data Association (PDA)

The problem with choosing the nearest or strongest neighbor is that, with some probability, sometimes it is not the correct measurement, because it has not been originated from the object in track, but it can be a false alarm or another target. Therefore, the filter will use (sometimes) incorrect measurements while "believing" that they are correct. This amounts to "overconfidence" and, even with moderate clutter density, it can lead to loss of the target [9], [17], [20].

The PDA algorithm calculates the association probabilities to the target being tracked for each validated measurement at the current time. This probabilistic or Bayesian information is used in the PDA tracking algorithm, which accounts for the measurement origin uncertainty. Since the state and measurement equations are assumed to be linear, the resulting PDAF algorithm is based on KF.

The approach suggested here is to obtain an estimator which incorporates all the measurements that might have originated from the object in track rather than selecting at each time one of them. The PDA algorithm calculates the association probabilities for each validated measurement at the current time to the target of interest. This probabilistic (Bayesian) information is used in the tracking PDA filter (PDAF) that accounts for the measurement origin uncertainty [9],[17], [20].

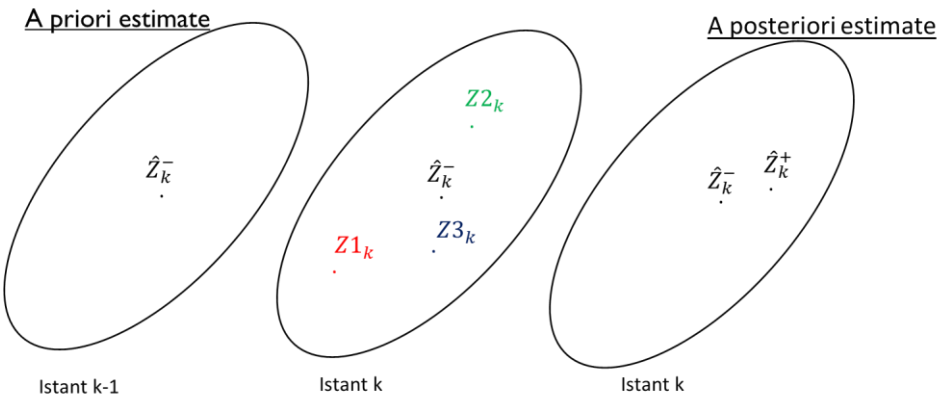

Fig. 2.8 PDAF Functionality

The PDAF uses a decomposition of the estimation with respect to the origin of each element of the latest set of validated measurements, denoted as

$$Z(k) = \{z_i(k)\}_{i=1}^{m(k)} \tag{2.7}$$

where $z_i(k)$ is the i-th validated measurement and $m(k)$ is the number of measurements in the validation region at time k.

The validation region is the elliptical region

$$V(k,\gamma) = \{z: [z_k - \hat{z}_k^-]^T S^{-1} [z_k - \hat{z}_k^-] \leq \gamma\} \tag{2.8}$$

where γ is the gate threshold.

The cumulative set (sequence) of measurements is

$$Z^n = \{z(j)\}_{j=1}^{n} \tag{2.9}$$

In view of the assumptions listed, the association events

$$\theta_i(k) = \begin{cases} \{z_i(k) \text{ is the target originated measurement}\} & i=1,\dots m(k) \\ \{\text{none of the measurements is target originated}\} & i=0 \end{cases} \quad (2.10)$$

are mutually exclusive and exhaustive for $m(k) \geq 1$

The conditional mean of the state at time *k* can be written as

$$\hat{s}_k^+ = \sum_{i=0}^{m(k)} \hat{s}_{ik}^+ \beta_i(k) \quad (2.11)$$

where

- $\hat{s}_{ik}^+$ is the updated state conditioned on the event that the *i*-th validated measurement is correct.
- $\beta_i(k) \triangleq P\{\theta_i(k) \mid Z^k\}$ is the conditional probability of this event (the association probability), obtained from the PDA procedure.

The estimate conditioned on measurement *i* being correct is

$$\widehat{s_{ik}^+} = \hat{s}_k^- + K_k v_i(k) \quad (2.12)$$

where the corresponding innovation is

$$v_i(k) = z_i(k) - \hat{z}_k^- \quad (2.13)$$

and the gain K_k is the same as in the standard filter

$$K_k = P_k^- C_k^T (S_k)^{-1} \quad (2.14)$$

For $i = 0$, if none of the measurements is correct, or, if there is no validated measurement $(m(k) = 0)$, it is

$$\hat{s}_0^+ = \hat{s}_k^- \quad (2.15)$$

so the update state equation for the PDAF is

$$\hat{s}_k^+ = \hat{s}_k^- + K_k v(k) \tag{2.16}$$

where the combined innovation is

$$v(k) = \sum_{i=1}^{m(k)} \beta_i(k) v_i(k) \tag{2.17}$$

and the association probabilities are

$$\beta_i(k+1) = \frac{e_i}{b + \sum_{j=1}^{m(k+1)} e_j} \quad i = 1, \ldots, m(k+1) \tag{2.18}$$

$$\beta_i(k+1) = \frac{b}{b + \sum_{j=1}^{m(k+1)} e_j} \qquad i = 0 \tag{2.19}$$

where

$$e_i = e^{-\frac{1}{2} v_i(k+1)^T S(k+1)^{-1} v_i(k+1)} \tag{2.20}$$

$$b = \left(\frac{2\pi}{\gamma}\right)^{\frac{n_z}{2}} m(k+1) c_{n_z}{}^{-1} \frac{1 - P_D P_G}{P_D} \tag{2.21}$$

The covariance associated with the updated state is

$$P_k^+ = \beta_0(k) P_k^- + [1 - \beta_0(k)] P_k^{c+} + \tilde{P}_k \tag{2.22}$$

where the covariance of the state updated with the correct measurement is

$$P_k^{c+} = P_k^- - K_k S_k K_k^T \tag{2.23}$$

and the spread of the innovations term is

$$\tilde{P}_k \triangleq K_k \left[\sum_{i=1}^{m(k)} \beta_i(k) v_i(k) v_i^T - v(k) v^t(k)\right] K_k^T \tag{2.24}$$

2.5.1 Joint Probabilistic Data Association Filter (JPDAF)

One of the limitations of PDAF is that it assumes that each target is isolated from all other targets and that false alarms present in the region of validation are modeled through a Poisson distribution.

However, it is possible that the interference is due not only to the presence of the false alarms within the gate, but also of other targets, in addition to the one of interest.

The following are the assumptions of the JPDA:

- There is a known number of established targets in clutter
- Measurements from one target can fall in the validation region of a neighboring target
- The past is summarized by an approximate sufficient statistic
- The states are assumed Gaussian distributed with means and covariances
- Each target has a dynamic and a measurement model

This is a target-oriented approach and extends the PDAF to a known number of targets, whose tracks have been established. Finally, it evaluates the measurement-to-target association probabilities for the latest set of measurements and then combines them into the state estimates [9], [23], [24].

The key feature of the JPDA is that it evaluates the conditional probabilities of the following joint association events

$$A(k) = \bigcap_{j=1}^{m} A_{jt_j}(k) \tag{2.25}$$

pertaining to the current time k, where $A_{jt}(k)$is the event that measurement j at time k originated from target t, j =1,…m, t=0,1,… N_t ; t_j is the index of the target to which measurement j is associated in the event under consideration and N_t is the known number of targets.

JPDAF consists of the following steps:

- The measurement-to-target association probabilities are computed jointly across the targets

- The association probabilities are computed only for the latest set of measurements — this is a non-backscan approach
- The state estimation is done separately for each target as in the PDAF

2.5.1.1 Cheap PDAF and Cheap JPDAF

In the standard PDA and JPDA, the association probabilities are calculated by considering every possible hypothesis as the association of the new measurements with existing tracks. Both approaches updates each track with a weighted average of all the measurements with which it can be associated, the weighting factor being the probability of association of the track with the measurement in question. Unfortunately, when these methods are generalized to the multi-target case, the computation of the probabilities is quite complex, increasing substantially the computational cost of the algorithm.

To overcome this issue, an ad-hoc PDA and JPDA formulation, commonly known as the Cheap PDA (CPDA) and Cheap JPDA, provides a good approximation of the association probabilities [25]-[27],

$$\beta_{tj} = \frac{G_{ij}}{S_{ti} + S_{rj} - G_{ij} + B} \tag{2.26}$$

where

- B is a constant which depends on clutter density (usually with B = 0, the algorithm works well)
- G_{tj} is proportional to the Gaussian likelihood function indicating the closeness of fit of target t with jth observation and it is given by:

$$G_{tj} = \frac{1}{|S_{tj}(k)|} exp^{[-\frac{1}{2} v_i(k+1)^T S(k+1)^{-1} v_i(k+1)]} \tag{2.27}$$

- S_{ti} is the sum of all G's for track *i*
- S_{rj} is the sum of G's for return *j*.

When updating the state of the target, only three measurements with the highest probability should be used, but this limitation is stated as a processor loading consideration. Another reason for limiting the number of measurements could be that the ad hoc probability may give a too high weighting to incorrect measurements and cause the covariance matrix to grow uncontrollably in a dense target environment.

However, the cheap versions of PDAF and JPDAF can be considered a smaller variety of the standard version of same algorithms, because they does not consider all the measures within the gate as likely candidates to the association procedure. As a consequence, this can lead to inaccuracies in the estimation of the target state, because the selected measures, within the gate, with higher probability could not be associated with the target of interest, but with the clutter or even to other targets.

2.6 Multiple Hypothesis Tracking (MHT)

Since most surveillance systems must track multiple targets, multiple target tracking (MTT) is the most important tracking application. Fig. 2.9 shows the basic elements of a typical MTT system [9], [19].

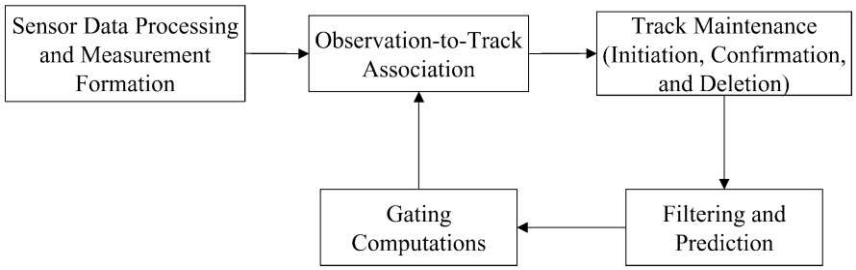

Fig. 2.9 Typical MTT system

The Multiple Hypothesis Tracker (MHT) evaluates the probabilities that there is a sequence of measurements originated from a target and this is valid for each measurement sequence. The MHT is a measurement-oriented approach,

so it does not assume a known number of targets and it also has track initiation capability.

This algorithm splits the existing track, whenever an association ambiguity is present and follows each branch (sequence of measurements) with a probability calculation.

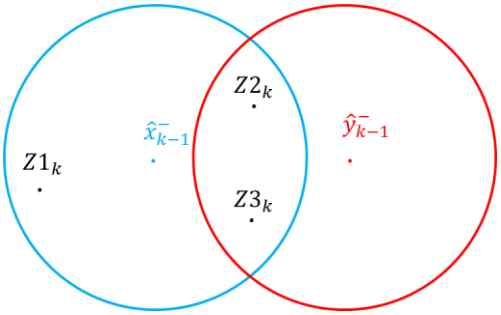

Fig. 2.10 Association ambiguity

Let us assume that tracks have been formed from previous data and a new set of input observations becomes available: this input observations are considered for inclusion in existing tracks and for initiation of new tracks. When closely spaced targets produce closely spaced observations there will be conflicts such that:

- there may be multiple observations within a track's gate;
- an observation may be within the gates of multiple tracks.

Fig. 2.10 shows a typical conflict situation in which track gates are placed around the predicted positions ($\hat{x}_{k-1}^-$, $\hat{y}_{k-1}^-$) of two tracks, and three measurements ($Z1_k$, $Z2_k$, $Z3_k$) satisfy the gates of either (or both) of the tracks. The global nearest neighbor (GNN) approach finds the best association of this measurement to existing tracks, which for example, would probably be $Z1_k$ to track $\hat{x}_{k-1}^-$ and $Z2_k$ to track $\hat{y}_{k-1}^-$. The term global indicates that the assignment is made considering all possible (within gates) associations under the assumption that an observation was produced by a single target. This distinguishes GNN from the nearest neighbor (NN) approach in which a track is updated with the closest observation even if that

observation may also be used by another track. Only those tracks that are included in the best assignment are kept, while, unassigned observations, in this case $Z3_k$, initiate new tracks. The assumption that an observation was produced by a single target is inherent in the standard GNN assignment. Tracks that do not share any common observations will be defined compatible, thus only this kind of tracks can appear in the same assignment solution.

2.7 Interactive Multiple Model (IMM)

The IMM adaptive estimation approach is based on the fact that the behavior of a target cannot be characterized at all times by a single model, but a finite number of models can adequately describe its behavior in different regimes [9], see Fig. 2.11.

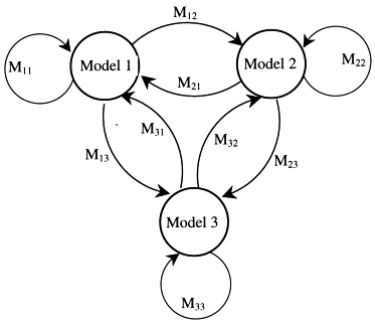

Fig. 2.11 General functionality of IMM

The IMM algorithm runs many Kalman Filters simultaneously based on several target models in an interacting manner. This model is governed by a discrete stochastic process, because it is one of a finite number of possible models (each corresponds to a behavior mode), that switches from one model (behavior mode) to another according to a set of transition probabilities (the dynamic Multiple Model (MM) approach). The value of hybrid models for tracking algorithms is that the occurrence of target maneuvers can be

explicitly included in the kinematic equations through switching through one model to another.

3

Validation of tracking algorithms on simulated data

3.1 Data characteristics

For the purpose of a greater understanding of the Kalman filter, an algorithm for the simulation of targets that move along a random two-dimensional trajectory and change direction has been implemented. Moreover, within this scene, false alarms were inserted randomly, following the Poisson distribution.

More in detail, in the generation of simulated data, used to validate the algorithms, the following two scenarios were considered:

1. in the case of single tracking, a two-dimensional x-y scenario with one target point type, distinguishing between cases of presence and absence of false alarms;
2. in the case of multi tracking, a two-dimensional x-y scenario with two targets point type, going to directly investigate the case of presence of the false alarms.

The two tracking algorithms used, the NNSKF and Cheap PDAF / JPDAF, were applied to these two scenarios.

In the initialization phase of both the algorithms, certain parameters were defined, as denoted in Tab. 3.1.

Parameter	Unity measure
Scene dimension	Matrix of 512x512 pixels
Pixel spacing	1.75 m
Antenna rotation period	2.4 s

Tab. 3.1 Main parameters

Subsequently, the input control and measurement matrices, known as the state transition matrices that will be necessary to update the status of the target, were defined. It is worth recalling that the Kalman filter, used to predict the state of a moving target on the surface of the sea, recalls the more general problem of a state estimation of a discrete-time process.
For the estimation procedure, the random variables representing

- the noise process, which corresponds to the sudden and abrupt changes of movement and acceleration of the target
- the measurement noise due to all those environmental signals that are not related to target

were assumed to be independent, white and with normal probability distribution.
For this reason, these problems related to the initialization of these parameters have been addressed, so as to make them as lifelike as possible if considered in a real system.
In this implementation of these filters, it was considered appropriate to calculate the covariance matrix of the measurement noise and process noise before the filters operations were carried out: for this purpose, it was necessary a calibration phase of such parameters. In addition, the initial velocities along the x and y directions have been placed at zero, since they are not known, while the initial positions of the targets along the x and y directions have been updated with the first positions received by the first simulation, to which a Gaussian random noise was added.
After setting the initial parameters, the simulation has been started and, simultaneously, both the algorithms have been run for validation.

3.2 The clutter model

Whatever the radar system and its task, it is necessary to have the exact knowledge of its characteristics (capabilities and limitations), in order to

correctly interpret the information it provides and not incur in false estimations.

A nautical radar receives backscattered signals arising not only from the targets of interest, but also from the sea surface (according to the mechanisms of backscattering) and from any precipitation. These echoes are added to the simulated radar images and affect the performance of the indicator, possibly even impairing the identification of targets. Such a kind of signal is conventionally denoted as *clutter*, because it always represents an unwanted signal (noise) that is superimposed on the useful signal and reduces the ability to detect targets.

For these reasons, in radar systems, a device, called anti-clutter, is always present and allows to filter this noise contribution.

The motion of the waves follows the wind direction, so this thickening is more significant towards the direction of origin of the wind, for the effect shown in Fig. 3.1, and extends to an apparently larger distance where the wind speed and the "strength" of the sea are greater. The most serious consequence is to mask any targets present within a certain area.

Of course, it could be possible to take into account the effect of sea clutter by properly modifying the propagation model underlying the radar processing, but none of the mechanisms proposed to describe the sea clutter is fully satisfactory: the complexity of the nature of the sea, together with the difficulties present in the control experiments, makes the realization of a single model a real challenge [22].

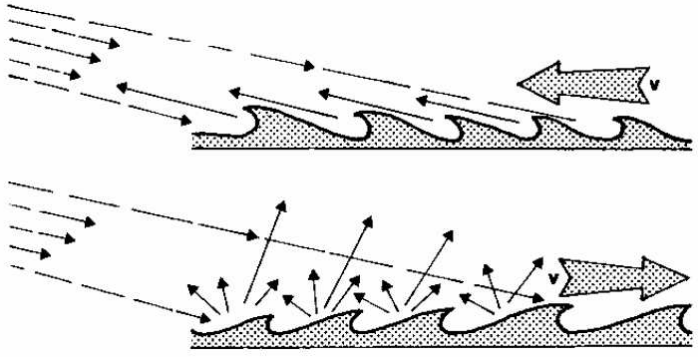

Fig. 3.1 Sea clutter origin (v, wind direction)

3.3 Model for false detection

False alarms are false positives and they can come from sensor imperfections or detector failures (clutter). They raise two fundamental questions:

- What is actually present inside the validation gate?
  - The real measurement?
  - A false alarm?
- How to model false alarms?

Let us assume that the sensor field of view V is discretized into N discrete resolution cells (or pixels), $c_i = 1, \dots, N$. A detection is declared in a cell if the output of the signal processor in this cell exceeds a certain threshold. Let us also assume that:

- the events of detection in each cell are independent of each other
- the occurrence of false alarms is a Bernoulli process with probability $p = P_F$.

Then, the probability mass function (pmf) of the number of false alarms in these N cells follows the binomial (Bernoulli) distribution

$$P\{n_{FA} = m\} = \mu_{FA}(m) = \binom{N}{m} p^m (1-p)^{N-m} \tag{3.1}$$

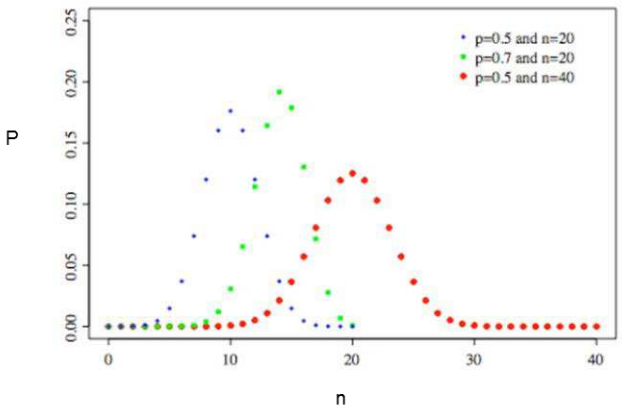

Fig. 3.2 Binomial distribution of false alarms

Let the spatial density λ be the number of the false alarms over the entire space

$$\lambda = \frac{E[n_{FA}]}{V} = \frac{Np}{V} \quad [occurrences\ per\ m^2] \tag{3.2}$$

Let us now consider the limiting case $N \rightarrow +\infty$, that is we reduce the cell size until the continuous case. Then, the Binomial becomes a Poisson distribution with

$$\mu_{FA}(m) = e^{-Np} \frac{(Np)^m}{m!} \tag{3.3}$$

Therefore the pmf of the number of false alarms or clutter points in the volume V, in terms of their spatial density λ, is given by

$$\mu_{FA}(m) = e^{-\lambda V} \frac{(\lambda V)^m}{m!} \tag{3.4}$$

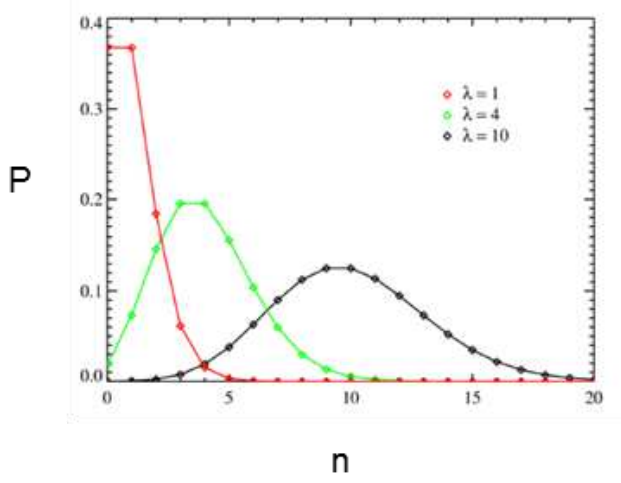

Fig. 3.3 False alarms distribution in function of their spatial density

This serves as justification for the common use of the Poisson distribution for the number of false measurements in a certain volume under the two assumptions given above.

The spatial distribution of the false alarms is uniform, thus, neglecting the granularity due to the resolution cells, the probability density function (pdf) of the location of a false alarm is

$$p(z|z\ is\ a\ false\ alarm) = \frac{1}{V} \tag{3.5}$$

where V denotes now the volume of the subspace in which the measurement is known to lie. Depending on the situation considered, this can be the sensor's surveillance region or a target's validation region [35].

3.4 Single target tracking

Initially, the case of application of KF and the Cheap PDAF in a scenario in the absence of false alarms is shown. The trajectory of the target estimated by the algorithms in three different instants of time is illustrated in Fig. 3.4a-c, respectively.

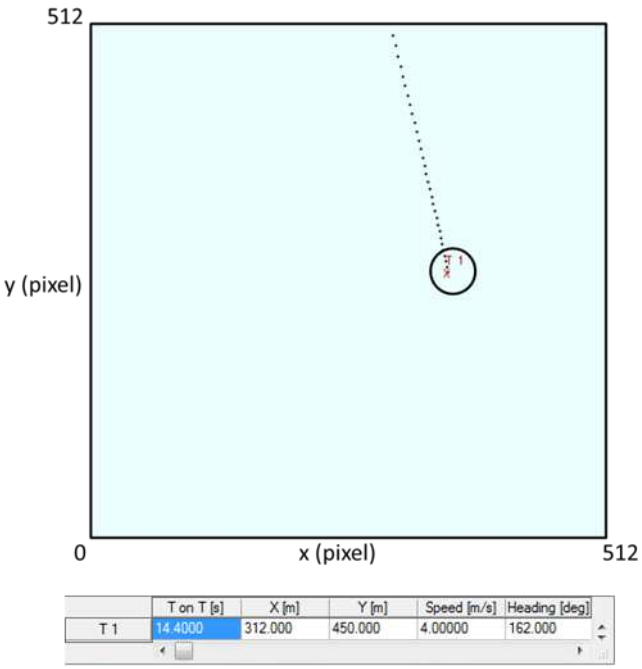

Fig. 3.4a Single target without clutter (acquisition time t1)

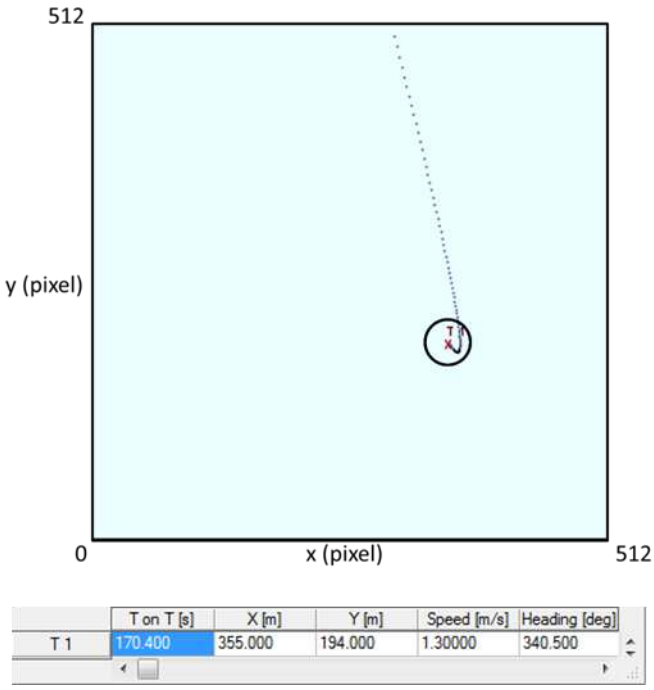

Fig. 3.5b Single target without clutter (acquisition time t2)

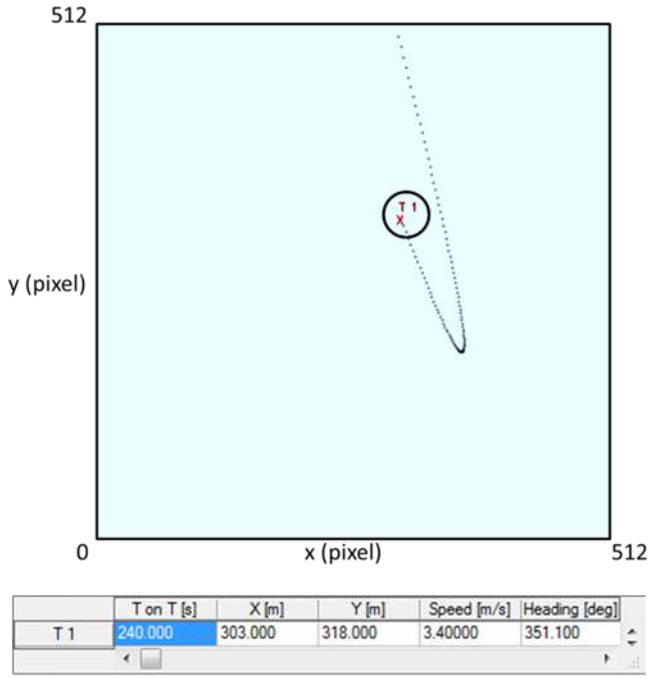

Fig. 3.6c Single target without clutter (acquisition time t3)

In each figure a table reporting the current state of various targets is given. In particular:

1. the first column represents the number of identified target;
2. the second column represents the Time on Target (T on T), which is how long the algorithm follows that particular target;
3. the third column represents the position X, in meters, of the identified target;
4. the fourth column represents the position Y, in meters, of the identified target;
5. the fifth column represents the magnitude of the velocity in meters / second, the identified target;
6. the sixth column represents the direction, in degrees, at which the target is moving, respect to the image center.

Of course, in case of absence of false alarms, the two algorithms are equivalent, since they both correctly follow the target.
Then we have considered a scenario where false alarms occurs. In the worst conditions, it has been assumed that, in each time instant k, three false alarms distributed randomly were present in the scene of observation, as well as the measure relative to the target. Therefore, for each time instant, four measures are present in the scene of analysis: three are false alarms and one will be the real one associated to the target of interest.
In the following, the trajectory of the target estimated by the two algorithms in three different instants of time is illustrated.

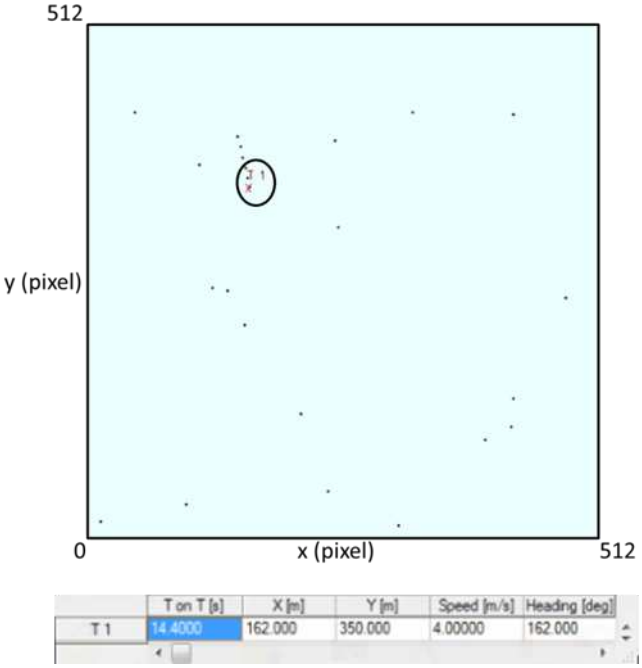

Fig. 3.7a Single target with clutter assuming 3 false alarms every time instant tracked with NNSKF (acquisition time t1)

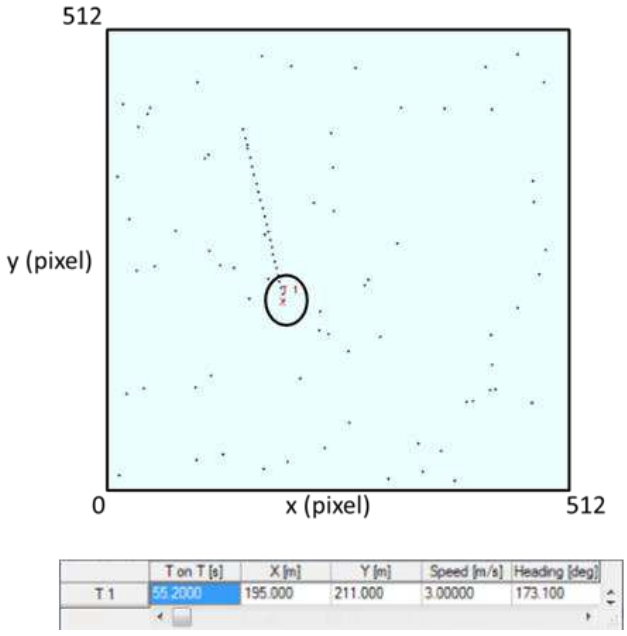

Fig. 3.8b Single target with clutter assuming 3 false alarms every time instant tracked with NNSKF (acquisition time t2)

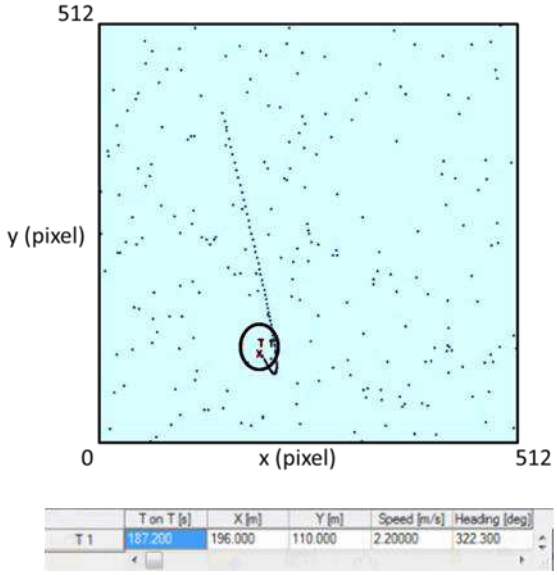

Fig. 3.9c Single target with clutter assuming 3 false alarms every time instant tracked with NNSKF (acquisition time t3)

In figures 3.5a-c, the trajectory of the single target T1 is correctly estimated, in fact the value of the T on T in the tables is always growing.

Subsequently, it was decided to further worsen the situation, working with 11 measures, 10 of which are false alarms and 1 measurement is really associated with the target.

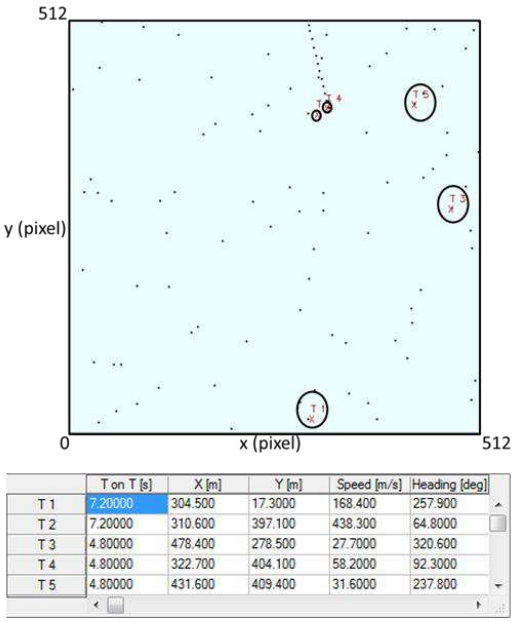

	T on T [s]	X [m]	Y [m]	Speed [m/s]	Heading [deg]
T 1	7.20000	304.500	17.3000	168.400	257.900
T 2	7.20000	310.600	397.100	438.300	64.8000
T 3	4.80000	478.400	278.500	27.7000	320.600
T 4	4.80000	322.700	404.100	58.2000	92.3000
T 5	4.80000	431.600	409.400	31.6000	237.800

Fig. 3.10a Single target with clutter assuming 10 false alarms every time instant tracked with NNSKF (acquisition time t1)

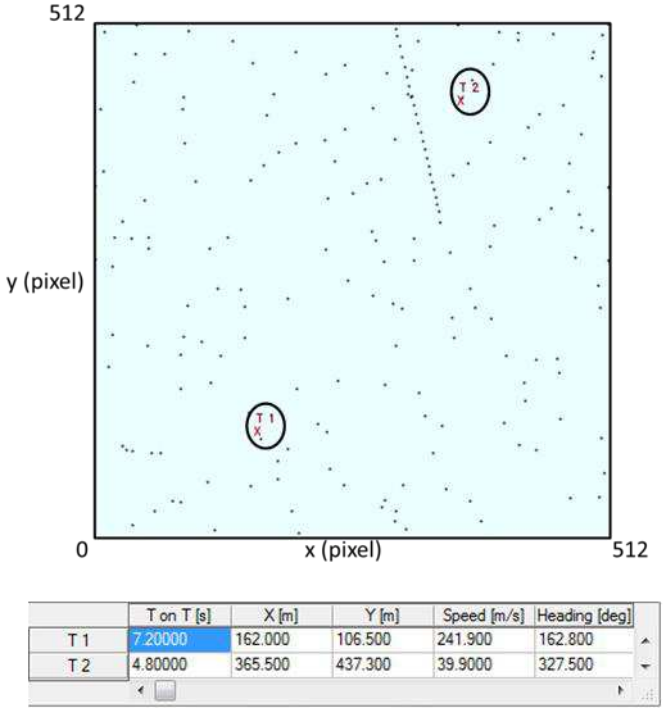

	T on T [s]	X [m]	Y [m]	Speed [m/s]	Heading [deg]
T 1	7.20000	162.000	106.500	241.900	162.800
T 2	4.80000	365.500	437.300	39.9000	327.500

Fig. 3.11b Single target with clutter assuming 10 false alarms every time instant tracked with NNSKF (acquisition time t2)

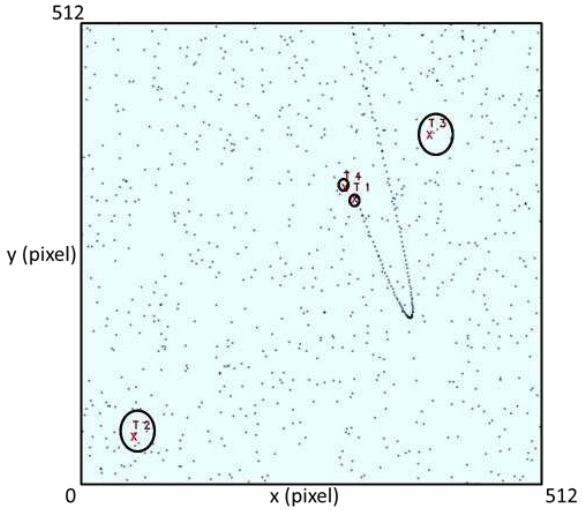

	T on T [s]	X [m]	Y [m]	Speed [m/s]	Heading [deg]
T 1	172.800	303.000	318.000	3.60000	353.200
T 2	7.20000	57.8000	54.2000	60.2000	343.400
T 3	4.80000	386.300	389.300	127.500	75.0000
T 4	4.80000	291.900	330.300	51.4000	104.700

Fig. 3.12c Single target with clutter assuming 10 false alarms every time instant tracked with NNSKF (acquisition time t3)

Figures 3.6a-c shows that the target T1 is followed by the tracking algorithm with some difficulties, in fact a consistence presence of false alarms can be noticed. Moreover, in Fig. 3.6b only two false alarms are present (one is named T1, as the target of interest, but it cannot be the target because it is completely outside the old trajectory), but, in this particular time instant, the trajectory is lost. Moreover, in figure 3.6c, in addition to the target of interest T1, also another target, T4, is detected near T1: this is due, essentially, to the problem concerning the association procedure; in particular, it is shown the case in which it wrongly attributes the origin of a measurement to the target of interest, since, among all the measurements present within that gate, one of these false alarms was also chosen as a measure originated from the target.

The following Figures 3.7a-c will show the validation of the Cheap PDAF on the same simulated data

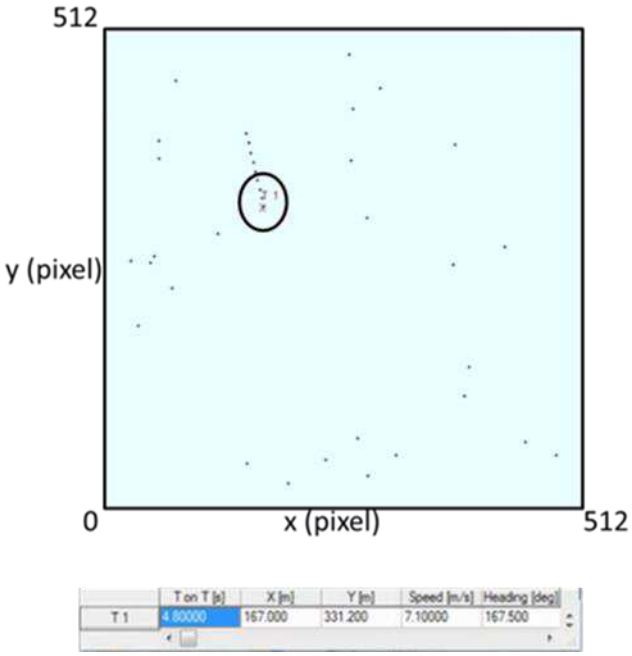

Fig. 3.13a Single target with clutter assuming 3 false alarms every time instant tracked with Cheap PDAF (acquisition time t1)

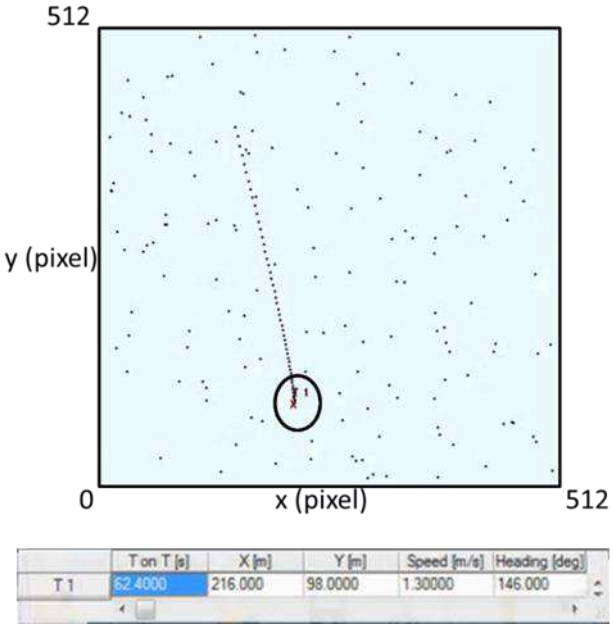

Fig. 3.14b Single target with clutter assuming 3 false alarms every time instant tracked with Cheap PDAF (acquisition time t2)

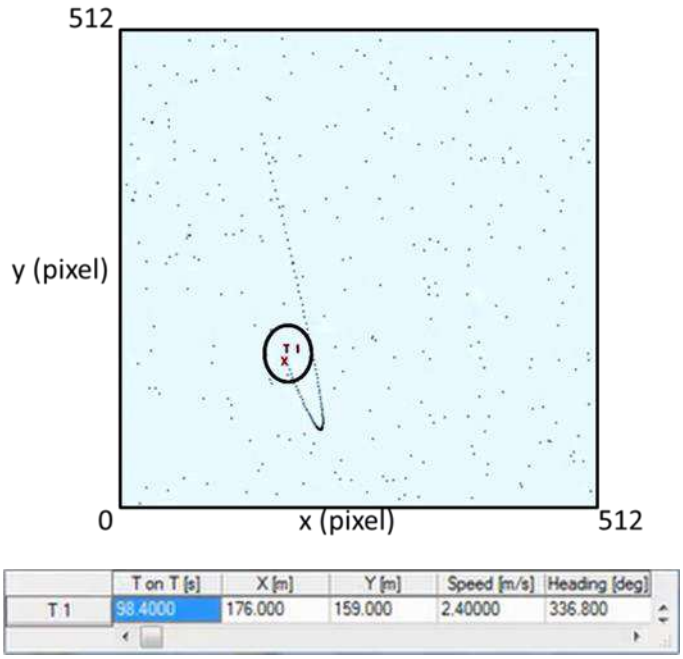

Fig. 3.15c Single target with clutter assuming 3 false alarms every time instant tracked with Cheap PDAF (acquisition time t3)

Also in this case, the target T1 is correctly tracked by the algorithm, regardless the presence of some false alarms. However, sometimes it is lost, in fact the

value of T on T related to this target is growing in Fig. 3.7a-b, but it is decreasing in Fig. 3.7c.

As in the NNSKF case, in the following figures we further complicate the problem, working with 11 measures, 10 of which are false alarms and 1 measurement is really associated with the target.

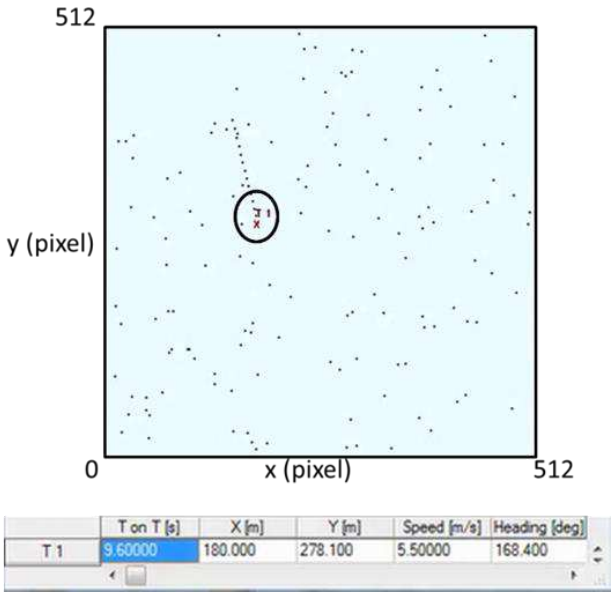

Fig. 3.16a Single target with clutter assuming 10 false alarms every time instant tracked with Cheap PDAF (acquisition time t1)

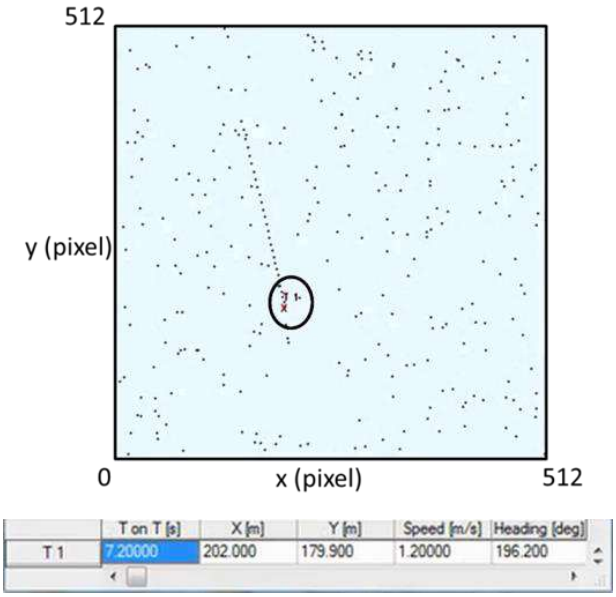

Fig. 3.17b Single target with clutter assuming 10 false alarms every time instant tracked with Cheap PDAF (acquisition time t2)

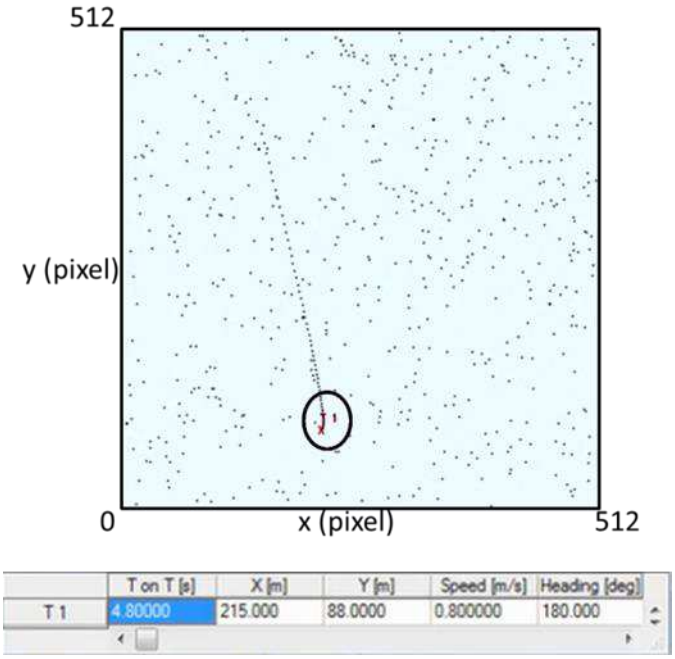

Fig. 3.18c Single target with clutter assuming 10 false alarms every time instant tracked with Cheap PDAF (acquisition time t3)

Figures 3.8a-c represents a situation similar to that shown on Fig. 3.7a-c, but in this case the presence of false alarms is very strong.

3.5 Multi target tracking

A scenario in presence of false alarms has been directly considered. As for the single target tracking case, in the worst conditions, it has been assumed that, in each time instant k, three false alarms distributed randomly were present in the scene of observation, as well as the measure relative to the target. Therefore, for each time instant, four measures are present in the scene of analysis: three are false alarms and one will be the real one associated to the target of interest.

In the following, the trajectory of the target estimated by the two algorithms in three different instants of time is illustrated.

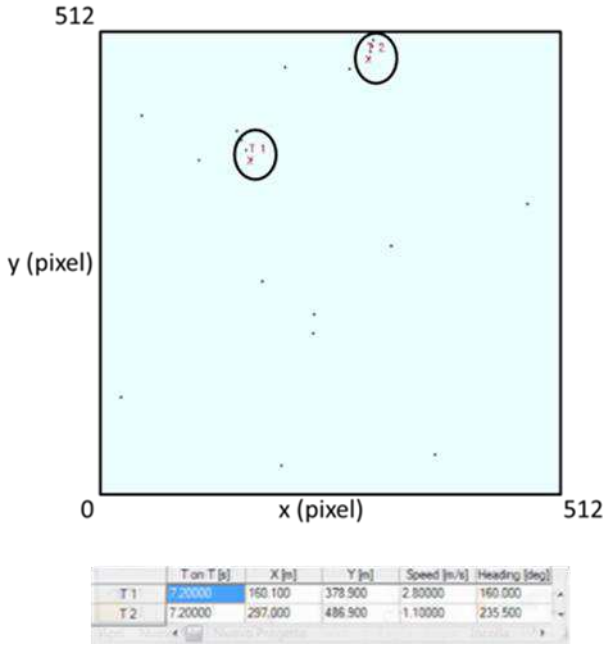

Fig. 3.19a Two targets with clutter assuming 3 false alarms every time instant tracked with NNSKF (acquisition time t1)

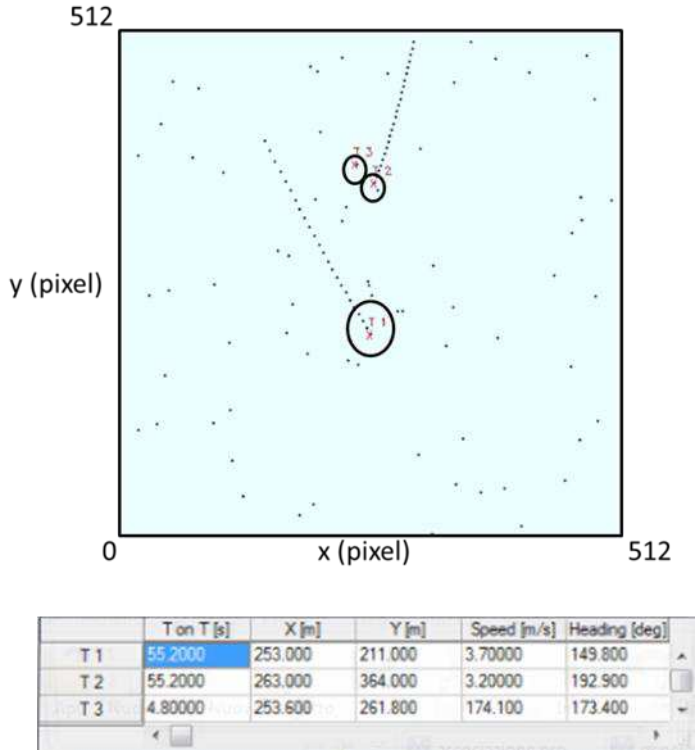

Fig. 3.20b Two targets with clutter assuming 3 false alarms every time instant tracked with NNSKF (acquisition time t2)

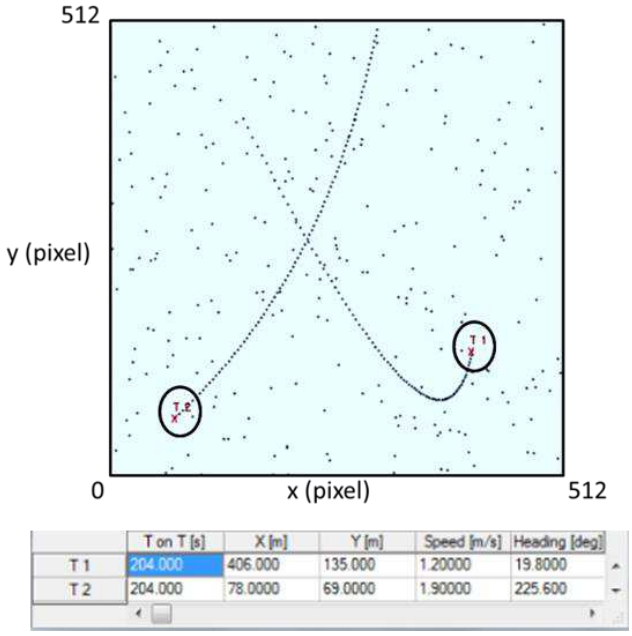

	T on T [s]	X [m]	Y [m]	Speed [m/s]	Heading [deg]
T 1	204.000	406.000	135.000	1.20000	19.8000
T 2	204.000	78.0000	69.0000	1.90000	225.600

Fig. 3.21c Two targets with clutter assuming 3 false alarms every time instant tracked with NNSKF (acquisition time t3)

Figures 3.9a-c shows that the trajectories of the two targets T1 and T2 are correctly estimated, in fact the value of T on T is always growing for both the targets.

As in the case of single target, in the following figures, it was decided to further worsen the situation, working with 11 measures, 9 of which are false alarms and 2 measurements are really associated with the targets.

In this case the situation is further complicated, because more targets moving in a scenario where the clutter is more present have to be tracked simultaneously.

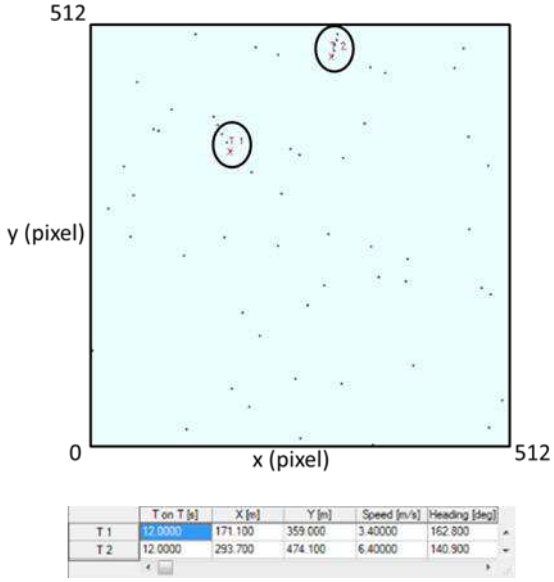

	T on T [s]	X [m]	Y [m]	Speed [m/s]	Heading [deg]
T 1	12.0000	171.100	359.000	3.40000	162.800
T 2	12.0000	293.700	474.100	6.40000	140.900

Fig. 3.22a Two targets with clutter assuming 10 false alarms every time instant tracked with NNSKF (acquisition time t1)

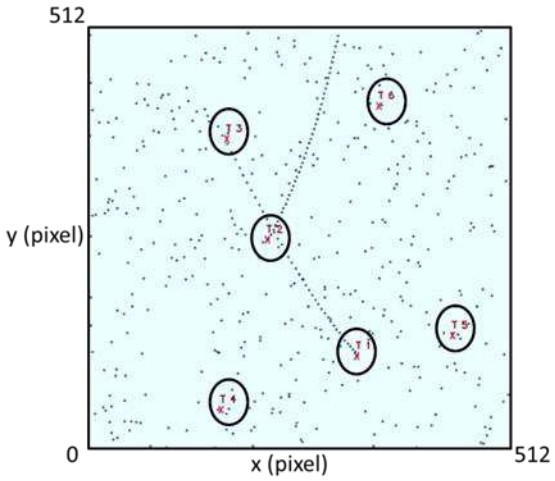

	T on T [s]	X [m]	Y [m]	Speed [m/s]	Heading [deg]
T 1	103.200	324.000	113.100	3.20000	156.400
T 2	103.200	216.000	254.000	1.50000	192.400
T 3	4.80000	167.500	376.000	276.300	355.600
T 4	4.80000	159.800	47.8000	223.400	260.500
T 5	4.80000	440.200	138.300	219.200	93.4000
T 6	4.80000	351.500	416.500	72.3000	107.900

Fig. 3.23b Two targets with clutter assuming 10 false alarms every time instant tracked with NNSKF (acquisition time t2)

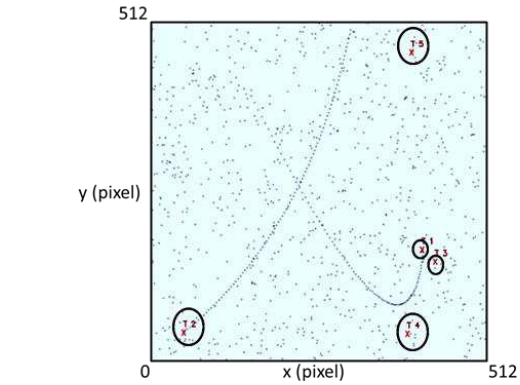

	T on T [s]	X [m]	Y [m]	Speed [m/s]	Heading [deg]
T 1	220.800	410.000	169.000	2.70000	347.200
T 2	220.800	49.0000	44.1000	3.70000	213.900
T 3	7.20000	430.100	151.200	361.300	125.700
T 4	4.80000	388.100	42.3000	144.300	113.400
T 5	4.80000	394.300	467.400	37.1000	122.400

Fig. 3.24c Two targets with clutter assuming 10 false alarms every time instant tracked with NNSKF (acquisition time t3)

Regardless of the presence of many false alarms, both the targets are correctly tracked by the algorithm (see Fig. 3.10a-c).

The following Figures 3.11a-c will show the validation of the Cheap JPDAF on the same simulated data.

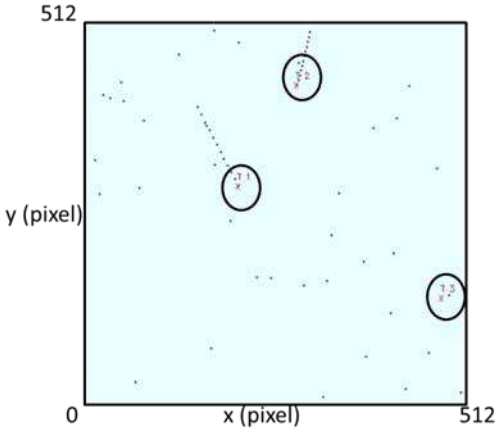

	T on T [s]	X [m]	Y [m]	Speed [m/s]	Heading [deg]
T 1	26.4000	200.000	304.000	4.50000	150.100
T 2	26.4000	285.100	436.000	2.70000	225.200
T 3	7.20000	172.900	79.4000	178.400	248.200
T 4	4.80000	500.500	22.1000	158.100	154.200
T 5	4.80000	204.400	486.300	28.1000	115.900

Fig. 3.25a Two targets with clutter assuming 3 false alarms every time instant tracked with Cheap JPDAF (acquisition time t1)

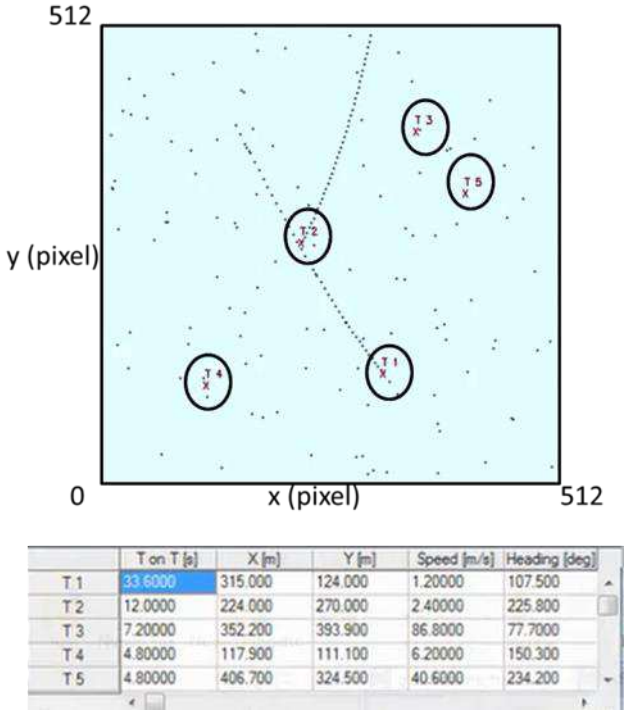

	T on T [s]	X [m]	Y [m]	Speed [m/s]	Heading [deg]
T 1	33.6000	315.000	124.000	1.20000	107.500
T 2	12.0000	224.000	270.000	2.40000	225.800
T 3	7.20000	352.200	393.900	86.8000	77.7000
T 4	4.80000	117.900	111.100	6.20000	150.300
T 5	4.80000	406.700	324.500	40.6000	234.200

Fig. 3.26b Two targets with clutter assuming 3 false alarms every time instant tracked with Cheap JPDAF (acquisition time t2)

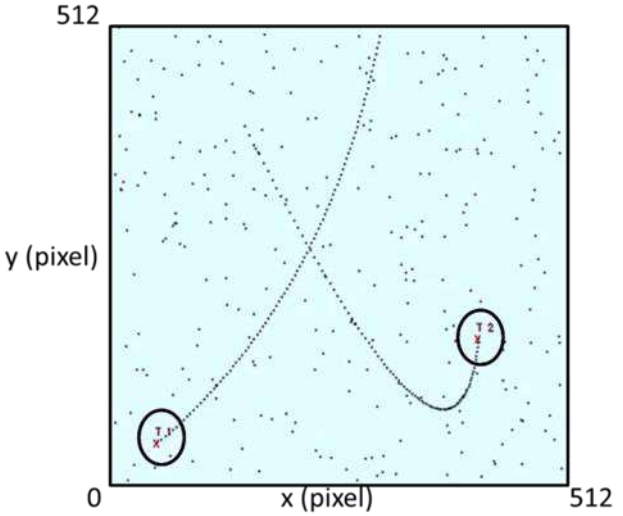

	T on T [s]	X [m]	Y [m]	Speed [m/s]	Heading [deg]
T 1	134.400	53.0000	48.0000	1.30000	246.200
T 2	14.4000	410.000	164.000	2.40000	19.2000

Fig. 3.27c Two targets with clutter assuming 3 false alarms every time instant tracked with Cheap JPDAF (acquisition time t3)

Figures 3.11a-c show that with some difficulties the targets are tracked, in fact sometimes T2 is lost because its T on T value is decreasing.

In the following figures, it was decided to further worsen the situation, working with 11 measures, 9 of which are false alarms and 2 measurements are really associated with the targets.

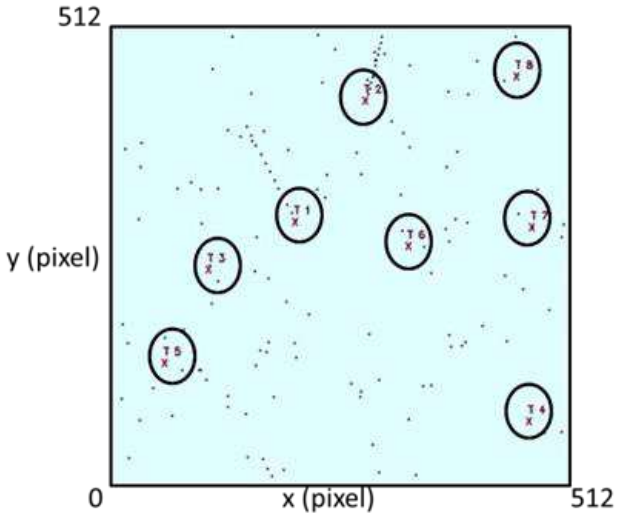

	T on T [s]	X [m]	Y [m]	Speed [m/s]	Heading [deg]
T 1	21.6000	205.000	294.900	3.00000	152.400
T 2	21.6000	282.900	430.000	2.30000	171.800
T 3	7.20000	108.900	242.100	77.9000	0.300000
T 4	4.80000	464.600	72.8000	29.3000	289.900
T 5	4.80000	59.8000	137.500	24.6000	25.8000
T 6	4.80000	331.100	268.400	53.3000	249.000
T 7	4.80000	468.100	288.700	32.4000	186.800
T 8	4.80000	450.700	456.900	12.4000	68.2000

Fig. 3.28a Two targets with clutter assuming 10 false alarms every time instant tracked with Cheap JPDAF (acquisition time t1)

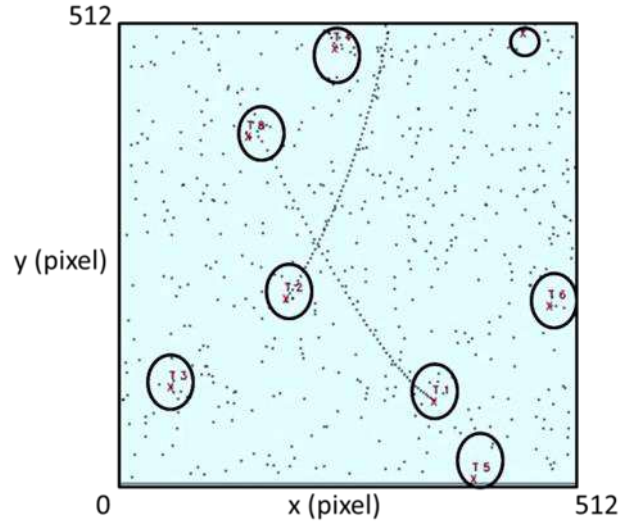

	T on T [s]	X [m]	Y [m]	Speed [m/s]	Heading [deg]
T 1	117.600	349.000	92.0000	0.300000	183.000
T 2	16.8000	191.000	210.000	1.40000	237.200
T 3	7.20000	500.200	364.600	190.800	195.600
T 4	4.80000	91.2000	147.100	7.50000	246.000
T 5	4.80000	227.500	449.700	25.7000	296.600

Fig. 3.29b Two targets with clutter assuming 10 false alarms every time instant tracked with Cheap JPDAF (acquisition time t2)

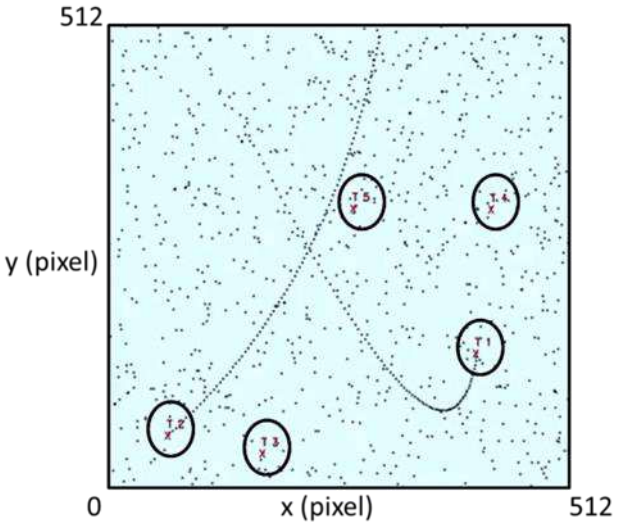

	T on T [s]	X [m]	Y [m]	Speed [m/s]	Heading [deg]
T 1	31.2000	407.000	144.100	0.600000	299.600
T 2	19.2000	70.0000	62.0000	2.60000	248.800
T 3	9.60000	137.000	427.200	268.900	247.900
T 4	7.20000	169.500	269.600	132.200	301.000
T 5	4.80000	448.400	171.300	20.7000	231.000

Fig. 3.30c Two targets with clutter assuming 10 false alarms every time instant tracked with Cheap JPDAF (acquisition time t3)

Figures 3.12a-c shows a very consistence presence of false alarms; nevertheless both the targets trajectories are correctly tracked by the algorithm.

3.6 Results and observations

The tests of the algorithms have confirmed the good results in the estimation of the trajectories of the two targets, despite the presence of false alarms. In fact, for all the algorithms, the important value to be considered is the Time on Target (T on T) reported in the tables present in every figure. For some tracks, this value is always increasing, so the target is correctly tracked. However, sometimes the T on T, for a particular target, switches from high values to small values because, in a fixed instant of time, the target was lost, therefore it had to be detected and tracked again by the tracking algorithms.

Subsequently, in the presence of false alarms, it may be noted how even the Kalman filter is able to follow a target with some little problematic. Once it is not clear what the target and once the target is even lost! This represents a limit of the Kalman filter.

To overcome this limitation, it was considered appropriate to use the variant of Cheap PDAF for single tracking and Cheap JPDAF for multi tracking. In particular, it was noted that the Cheap PDAF / JPDAF offers, for the same number of false alarms, performance comparable with those of the NNSKF.

4

X Band Radar Target Tracking in Marine Environment: a Comparison of Different Algorithms in a Real Scenario

4.1 Introduction to X-band radar

Typically, marine X-band radars are employed to detect targets on the sea surface during the navigation, but they can also provide information for both the sea state parameters, also during the night and in poor visibility conditions (e.g., in presence of fog). However, radar echoes arising from the sea surface, commonly considered as an undesired signal (clutter), as well as the interaction between the electromagnetic waves and the rain precipitations, can strongly affect the capability to detect the obstacles present during the navigation [30]. The data were acquired by the X-band radar system installed at the port of Giglio island during the removal operations of the Costa Concordia wreck and made available by the Consorzio Lamma that manages the system for research purpose. This system, called Wave Monitoring, provided by the Remocean S.p.A. company, has the purpose of measuring waves and surface currents analyzing the sea clutter received by the radar [48]-[53]. The X-Band radar system deployed in this study is operating at frequency of 9.5 GHz and its general characteristics are reported in Table 4.1.

Parameter	Value
Antenna rotation period	2.41 s
Range resolution (Δr)	7 m
Azimuth resolution ($\Delta\phi$)	0.9°
Radar scale	3072 m
View angular sector	260°
Polarization	HH
Peak power	25 kW

Tab. 4.1 Parameters of the acquisition system

This device allows us to obtain 2D spatial images of the scene of observation at different time instants. Figure 4.1 depicts a schematic configuration of the wave monitoring system for the coastal area:

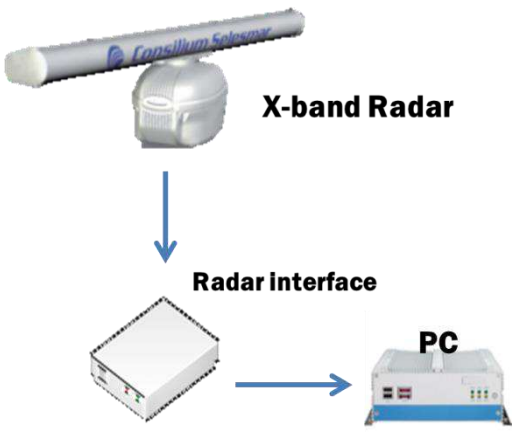

Fig. 4.1 Architecture of the acquisition and processing system of the radar data

The system architecture is very easy and flexible and is composed by a radar interface and an elaboration unit. The elaboration unit is an high performance industrial computer, designed to work in non-conventional environments, which is connected to the radar signals acquisition interface. The radar interface is an analog-to-digital (AD) converter for the received signal.

4.2 Validation of tracking algorithms on real data acquired by an X-band radar

After the analysis on simulated data, which has been also exploited to tune the algorithms with respect to the particular operative environment we are dealing with, the considered algorithms have been validated on real data.
In particular, a Consilium X Band Radar radiating a maximum power of 25 kW and equipped with a 9 feet (2.74m) long antenna was deployed. The radar antenna is located at the coordinates LAT=42°21'39.66"N; LON=10°55'16.31"E. The antenna is installed on a lighting pylon at a height of 15 m above sea level [48]-[53].

The following Figure shows the installation site of the radar:

Fig. 4.2 Installation site of the Remocean system indicated by the red circle

For this study, data acquired by the Remocean system were used for these different purposes as an input to the tracking algorithms and exploited them to monitor the movement of several targets that were populating the scene during the recovery operations.

In so doing, it has been possible to validate the algorithms in a real context, in which data are affected by the typical forms of clutter of the marine environment and are characterized by the presence of multiple moving targets. The following figure shows a radar image superimposed to the map of Giglio island, showing clutter and moving targets at this port.

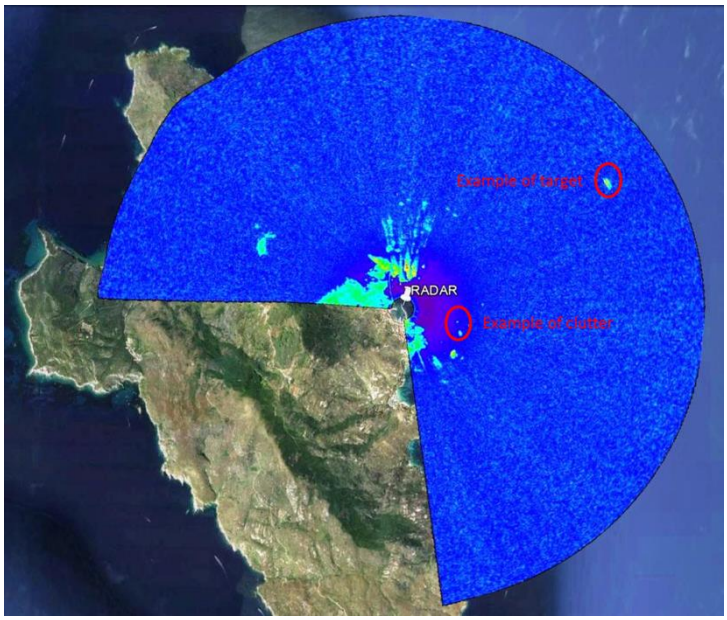

Fig. 4.3 Radar image showing clutter and moving targets at the port of Giglio Island

4.3 Clustering

Differently from what assumed in the algorithms, the targets are obviously extended ones and not modeled as point targets, as illustrated in the red circle in Fig. 4.4.

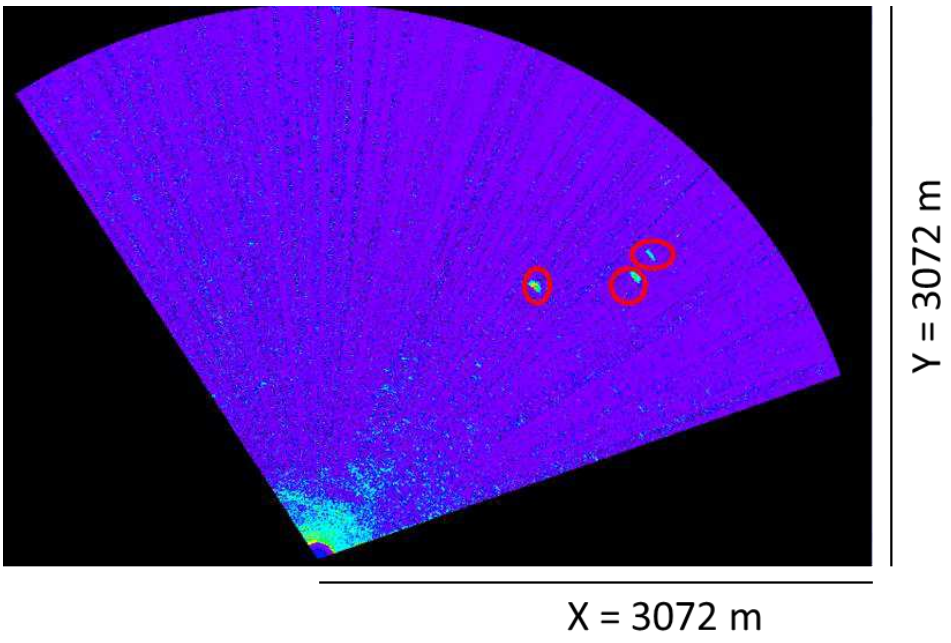

Fig. 4.4 Radar image with three targets indicated by the red circles

This is because, in a given time interval, the radar acquires many backscattered signals (i.e., many points), all referred to the same vessel. As a consequence, we had to use an extractor module (the yellow block in Fig. 4.5) to encompass such points in a single "cloud" through clustering and, subsequently, determine the center of gravity of such a cloud and track only this one.

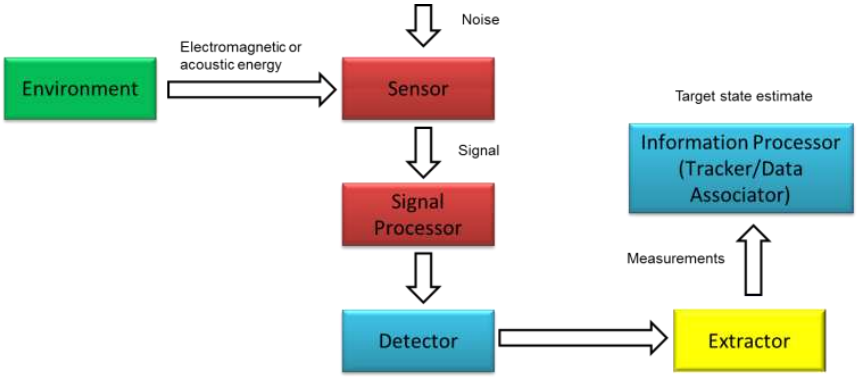

Fig. 4.5 Block diagram of a detection and tracking system

The clustering technique used is the bottom-up one and agglomerative, that is, initially, each element (leaf) is considered as an isolated cluster and then this technique continues to assemble common elements to the cluster until a fixed number of cluster is obtained.

4.4 K-distributed clutter

In general, noise is a random phenomenon, which is algebraically added to the useful signal coming from the target of interest, so it can increase or decrease the total signal received by the radar. The aim is to maximize the signal to noise ratio in order to maximize and optimize the analysis of the data provided by the radar. Typically, noise is well represented in probabilistic terms from a Rayleigh distribution, while the amount of signal and noise has a Gaussian probability density.

In our case, noise is also (and mainly) influenced by marine clutter, so that term is the need to determine probability distributions able to describe its experimentally properties. To this end, the scientific community to introduce new models of clutter, whose statistical characteristics are in better agreement with those found in practice with the Gaussian model, typically used as a statistical model to describe the noise evolution.

For example, because of the presence of spikes that characterizes the returns from the sea, the use of the Rayleigh random variable as a model to describe statistically the distribution of the amplitudes of the clutter is inappropriate. Rather, the use of heavy-tailed distributions, for which the probability to find isolated samples whose amplitude is relatively high in the return from the clutter is no longer negligible could be more appropriate.

For this purpose, the K-distribution is surely among the most used to describe the sea clutter because, by assigning an appropriate value to its parameters, it closely approximates the histograms of the amplitudes of the radar returns in different sea conditions, as well as allows effectively taking into account correlation properties of clutter [2], [7], [23]-[34].

Therefore, to statistically describe the clutter to the first order as a random, K–distributed, variable C, having shape-parameter v ($v > 0$) and scale-parameter b ($b > 0$), it means that the amplitude of the clutter returns have a probability distribution function (pdf) given by the following expression:

$$C \sim K(v,b) \Leftrightarrow f_c(c) = \frac{b^{v+1}}{\Gamma(v)} \frac{1}{2^{v-1}} c^v K_{v-1}(bc) \tag{4.1}$$

where Γ (□) is the Gamma Eulerian function and K_{v-1} (•) is the Bessel function of the second kind and order $v-1$.

As can be seen from Figure 4.6, the choice of the v parameter entails a change of shape in the pdf. In particular:

- the lower the value of this parameter ($v \rightarrow 0$), the slower the decay of the tail of the distribution (spiky clutter);

- on growing of v, incurring into spikes becomes increasingly unlikely and they tend to disappear altogether
    - for $v \rightarrow +\infty$, the limiting case for which the distribution K tends to the Rayleigh distribution.

Typically, values of v encountered in real data are such that v [0.1,+∞) [23], [24].

It is useful to observe that, in addition to being a good model for real data, assuming that the clutter C follows the distribution K (v, b) is suitable to a convenient and interesting physical interpretation.

In fact, said $C \cdot K(v,b)$ the random variable which describes the amplitude of the sea clutter, it appears that C can be expressed as

$$C = S\Sigma \tag{4.2}$$

where S and Σ are two independent random variables, such that S~Ray(1) and $\Gamma^2 \sim \Gamma\left(v, \frac{b^2}{2}\right)$ (compound gaussian model [24]-[26], [31], [32]). In other words, the precedent expression states that the pdf of a random variable $C \cdot K(v,b)$ can be expressed as (Theorem of Total Probability)

$$f_C(c) = \int_0^{+\infty} f_S(c \mid \sigma) f_\Sigma(\sigma) d\sigma = \int_0^{+\infty} \frac{c}{\sigma^2} \exp\left\{-c^2/2\sigma^2\right\} f_\Sigma(\sigma) d\sigma \tag{4.3}$$

i.e., that the received signal can be interpreted as the backscatter from a scene modeled as a two scales surface, where $S^2 \sim Exp(\sigma^2)$ represents the power of the return from the fast varying components of the surface (speckle, or the return from capillary waves), and whose average value σ^2 is locally modulated by slowly varying components of the same surface (the texture, that is, the backscattering coming from the long-wave) according to the distribution $\Gamma^2 \sim \Gamma(v, \frac{b^2}{2})$ [24]-[26].

Far from this assumption, it is assumed that the correlation characteristics of the clutter are dictated solely by the component of texture, whose correlation length (both in space and in time) is much greater than that of the speckle, which is therefore modeled as a white random process.

Such considerations are endorsed by empirical evidence, which shows that the returns from the capillary waves remain correlated in the order of milliseconds, while the gravitational waves have an average length of time correlation of the order of seconds [24].

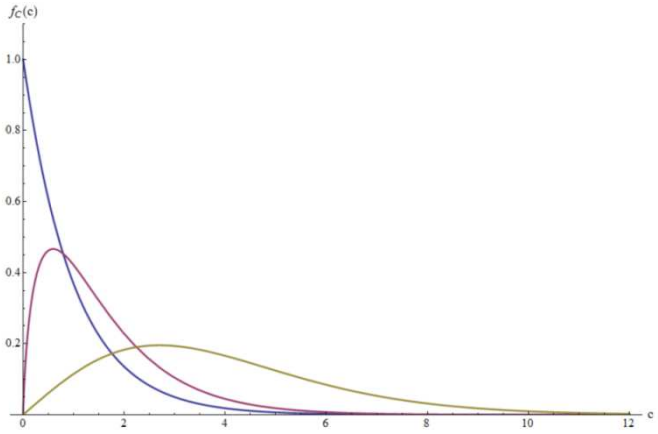

Fig. 4.6 Pdf of the K-distribution for $\boldsymbol{b}$ =1 and $\boldsymbol{v = 0.5}$ (blue), $\boldsymbol{v = 1}$ (violet) and $\boldsymbol{v = 5}$ (yellow)

4.5 Results and observations

This paragraph will show the results of the validation of the NNSKF and of the Cheap PDAF and JPDAF on real data acquired by a X-band marine radar. The following table shows the parameters used in the elaboration system for all the algorithms:

Parameter	Value
X scene dimension	1024 m
Y scene dimension	1024 m
False alarm probability	10^{-3}
Minimum distance between two ships to be distinguished	12 m
Gate radius	50 m

Tab. 4.2 Parameters of the elaboration system

Figures 4.7a-d show the validation of the NNSKF on real data already discussed. It can be seen that this algorithm correctly "follows" the trajectory of the three targets present in the upper right side of the observation scenario. The other targets on the lower side are false alarms, in fact they are not as extended as the three ones on the upper right side.

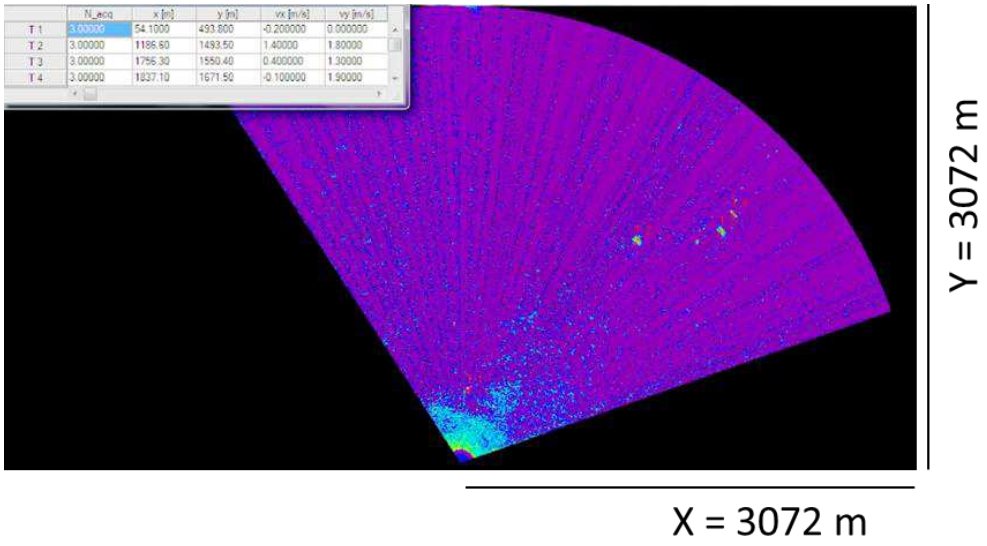

Fig. 4.7a Real data acquired by the X-band radar system tracked with NNSKF (acquisition time t1)

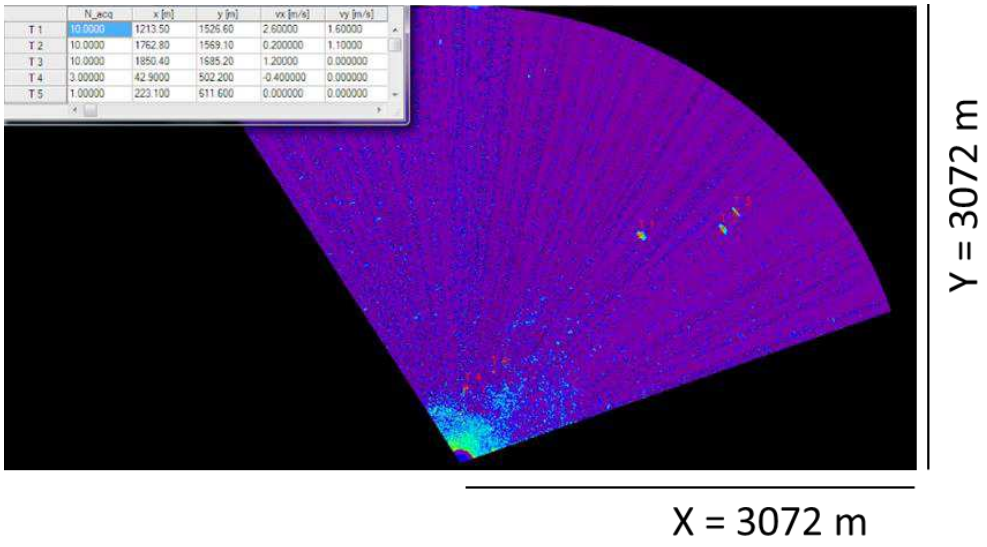

Fig. 4.8b Real data acquired by the X-band radar system tracked with NNSKF (acquisition time t2)

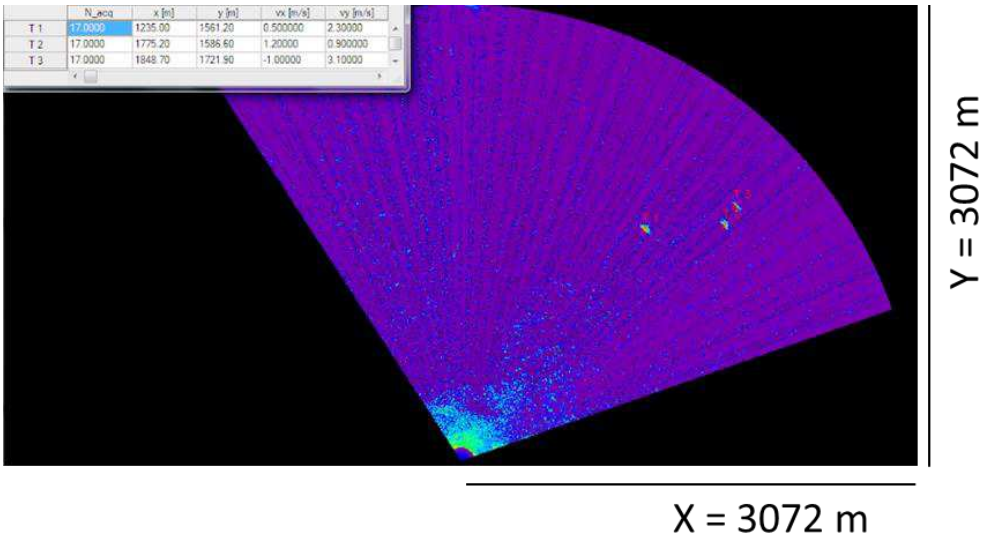

Fig. 4.9c Real data acquired by the X-band radar system tracked with NNSKF (acquisition time t3)

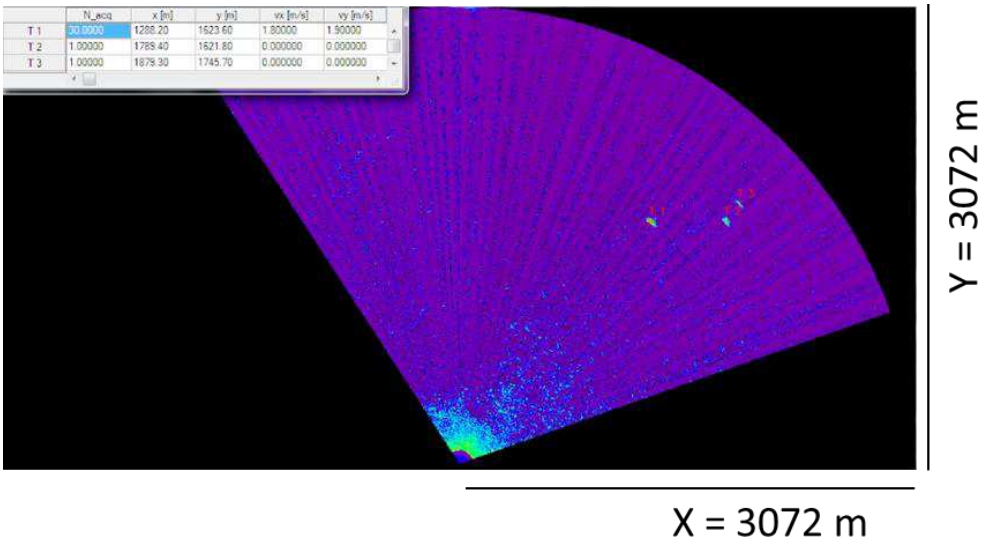

Fig. 4.10d Real data acquired by the X-band radar system tracked with NNSKF (acquisition time t4)

Figures 4.8a-d show the validation of the Cheap PDAF on the same real data. This algorithm presents some problems to track the state of the three targets, in fact in Fig. 4.8a only two targets are correctly tracked and, in the worst case, in Fig. 4.8c all targets are temporarily lost. This is due to the limitation of the Cheap PDAF, which is not suitable in multi-target scenarios.

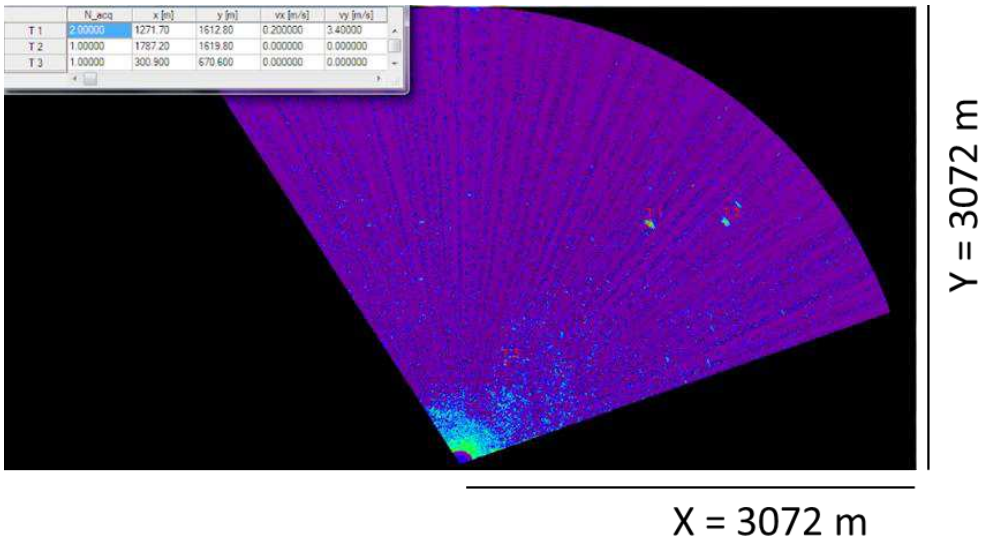

Fig. 4.11a Real data acquired by the X-band radar system tracked with Cheap PDAF (acquisition time t1)

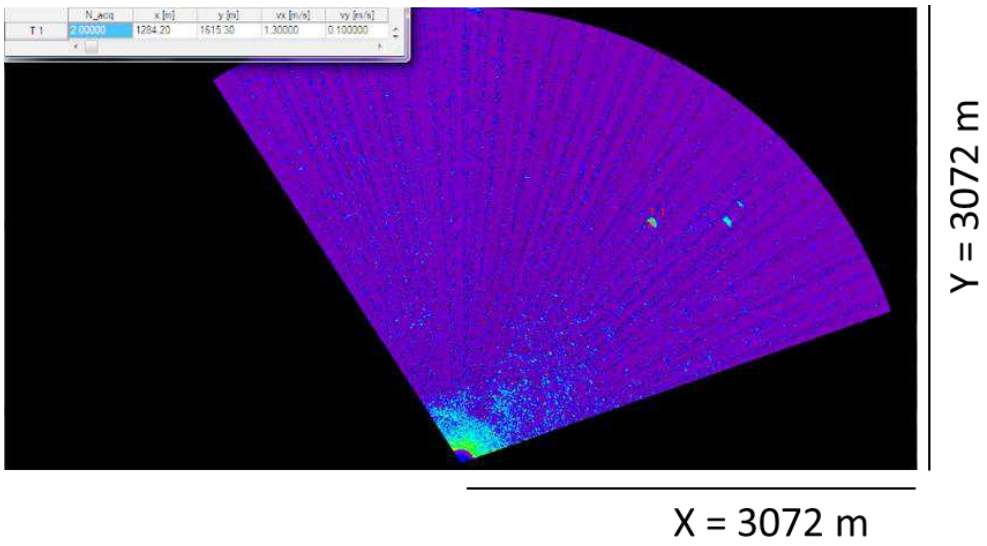

Fig. 4.12b Real data acquired by the X-band radar system tracked with Cheap PDAF (acquisition time t2)

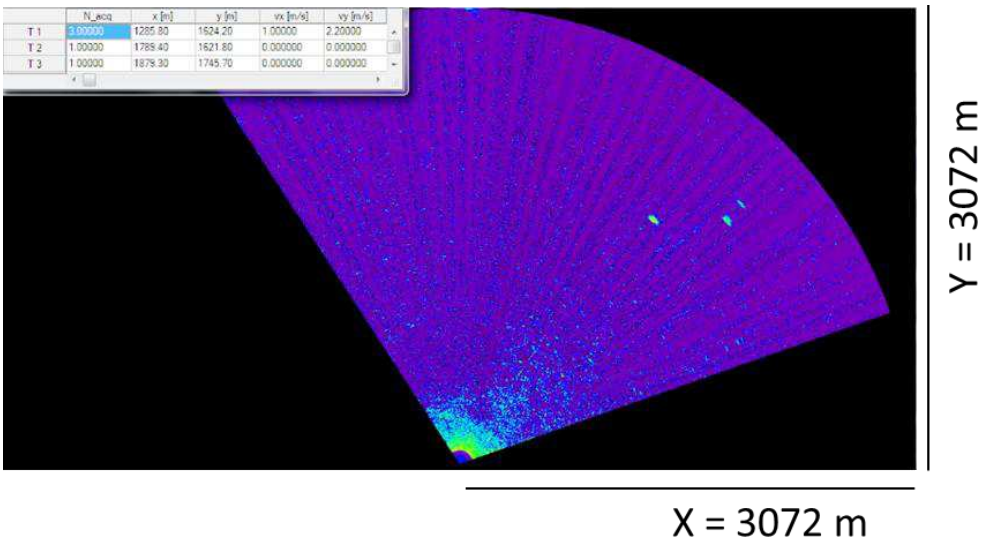

Fig. 4.13c Real data acquired by the X-band radar system tracked with Cheap PDAF (acquisition time t3)

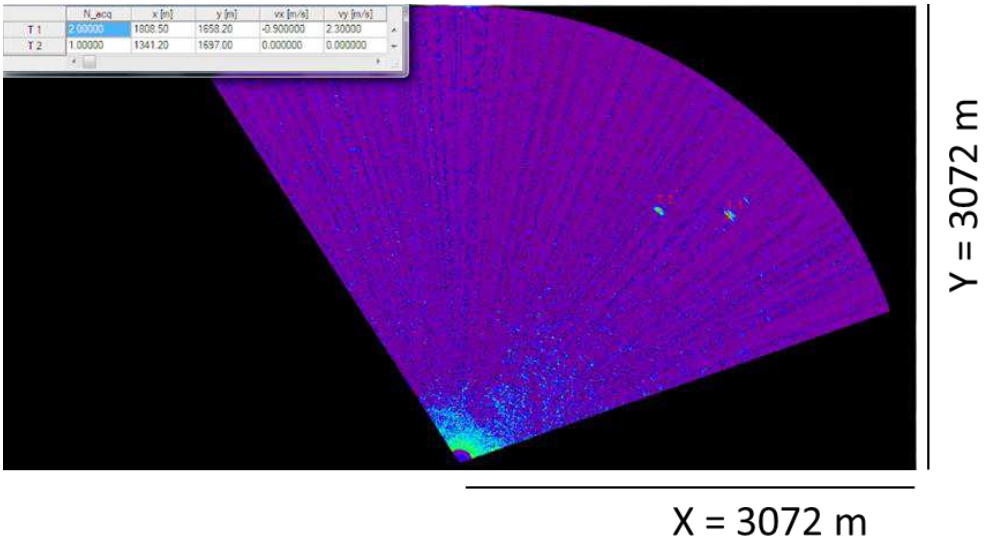

Fig. 4.14d Real data acquired by the X-band radar system tracked with Cheap PDAF (acquisition time t4)

Figures 4.9a-d show the validation of the Cheap JPDAF on the same real data. This algorithm perfectly estimates the state of the three targets, because it is particularly suitable in multi-target environments.

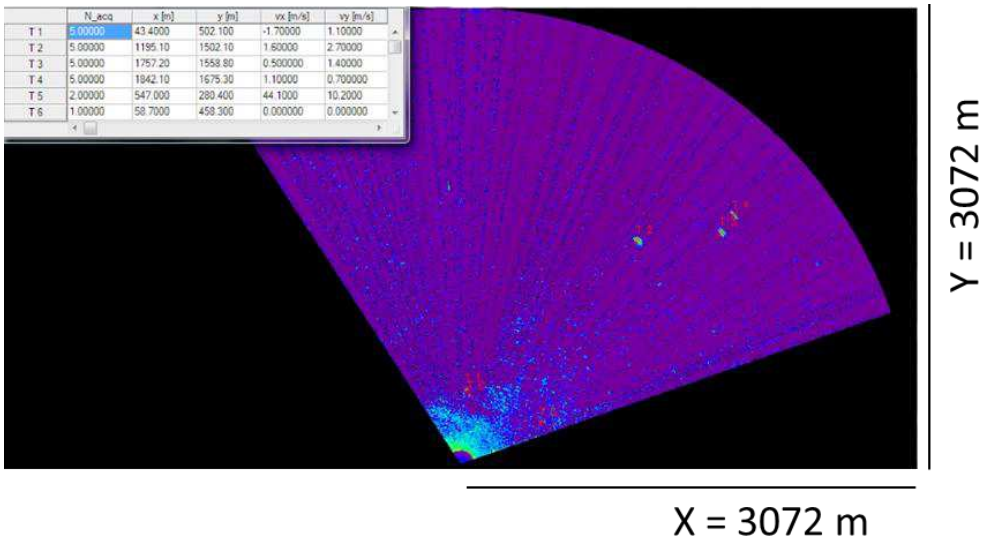

Fig. 4.15a Real data acquired by the X-band radar system tracked with Cheap JPDAF (acquisition time t1)

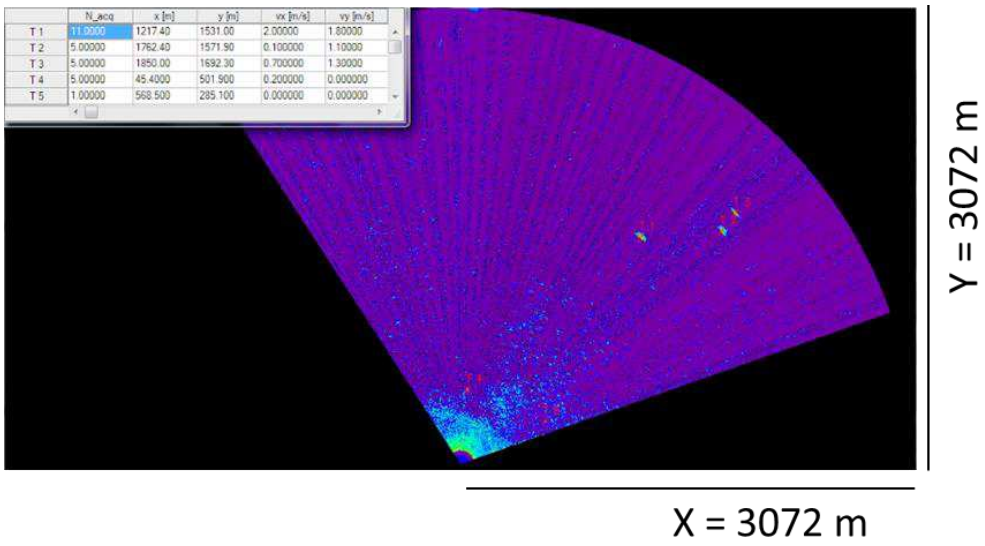

Fig. 4.16b Real data acquired by the X-band radar system tracked with Cheap JPDAF (acquisition time t2)

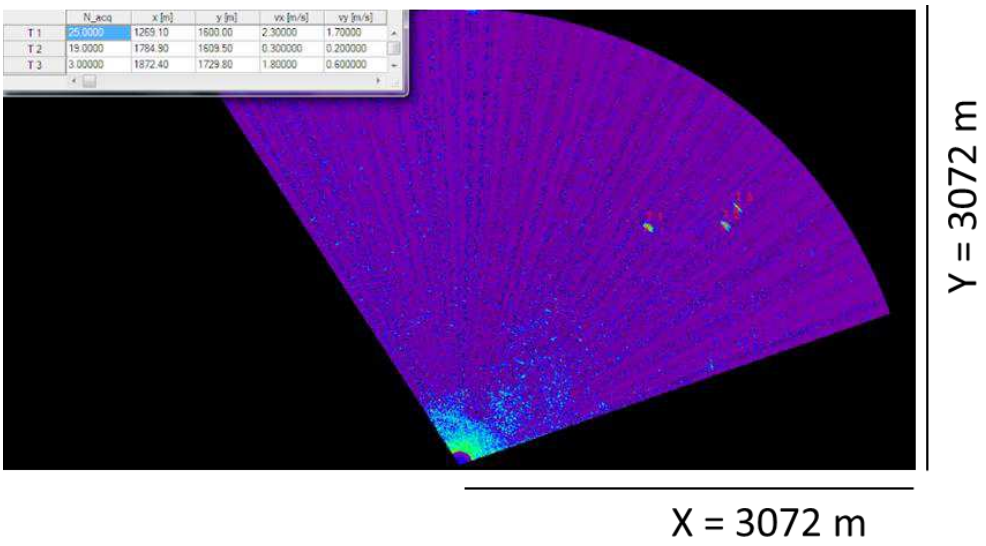

Fig. 4.17c Real data acquired by the X-band radar system tracked with Cheap JPDAF (acquisition time t3)

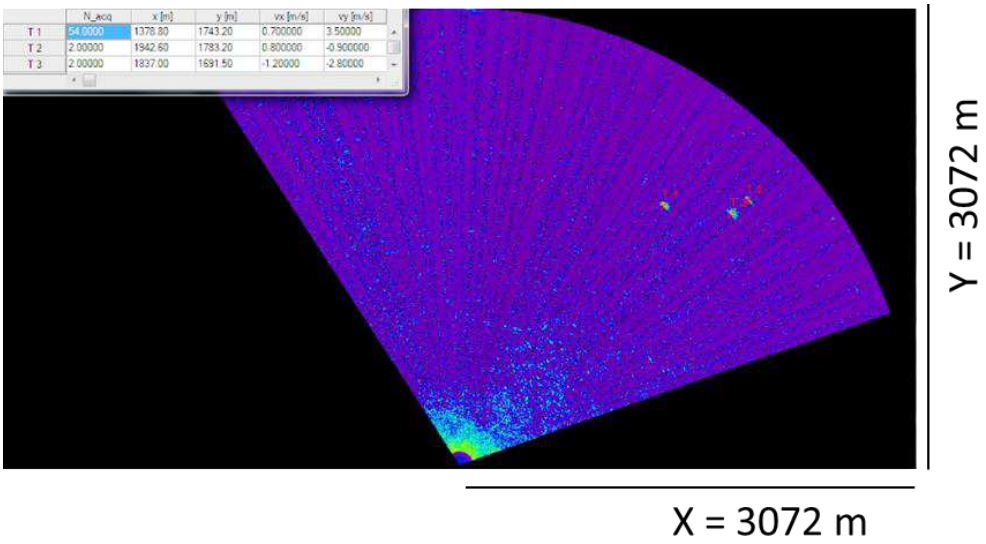

Fig. 4.18d Real data acquired by the X-band radar system tracked with Cheap JPDAF (acquisition time t4)

For all the algorithms, it can be seen that the value of Time on Target (T on T) reported in the tables present in every figure is always increasing, so the target is correctly tracked. However, sometimes the T on T, for a particular target, switches from high values to small values because, in a fixed instant of time, the target was lost, therefore it had to be detected and tracked again by the tracking algorithms.

The obtained results have confirmed that NNSKF is able to correctly predict the target tracks present in the scenario, even if sometimes the estimate is "corrupted" by the sea clutter. Conversely, the considered scenario was critical for Cheap PDAF, in which a high rate of false alarms was found and the track of the target was constantly lost. The cause of this behavior is to be found in the fact that one of the limits of the PDAF (and, consequently, of all its variants) is to assume that each target is isolated from all other targets and that it is assumed a Poisson distribution for the false alarms present in the validation region. Therefore, if within the gate, in addition to these false alarms and to the single target, also other targets close to each other begin to be present, the previous assumption is no longer valid since now the interference is due not only to the presence false alarms, but also to the presence of other targets, in addition to the one of interest.

Consequently, it was applied the Cheap JPDAF (Cheap Joint PDAF), more suitable for a multi-tracking scenario, as it considers the fact that in the gate, in addition to the measures associated with the target of interest, measurements associated to other targets can also be present, showing better results than the case of Cheap PDAF and comparable to NNSKF. The presence of another target is not necessary to the correct operation of the Cheap JPDAF; it means that this algorithm works well also with one target. However, if more than one target is present in the scenario of interest, the Cheap JPDAF is more suitable of the Cheap PDAF for the reasons already explained in par. 2.5.1.

5

Conclusions and future perspectives

The algorithms we have considered are the probabilistic data association filter (PDAF) variants called Cheap PDAF and Joint PDAF (JPDAF) for multi-tracking and the Kalman filter (KF) variant called nearest neighbor standard Kalman filter (NNSKF). These algorithms have been first analyzed using simulated data to understand the role played by the association procedure. From such analysis, we have been able to observe that when clutter begins to have a significant effect, the number of false alarms increases, so the NNSKF appears to be much less effective. As a matter of fact, in some time instants, the NNKSF wrongly attributes the origin of a measure to the target of interest. This was exactly the kind of uncertainty which arises during the data association, and is the core problem of target tracking. In fact, after the association procedure, the NNKSF algorithm considers that the selected measure is always associated with a target, although such a measure might be associated with a false alarm, or even to another target. This problem can then lead to the loss of the target and therefore the failure of the tracking procedure.

To overcome this limitation, it was considered appropriate to use the Cheap PDAF. This algorithm, among all the measurements present within the validation region, selects the one which has the highest probability of association, i.e., the one that is "more likely" to have been originated from the target of interest. However, if, within the gate, there is another target close to the target of interest, the interference not only arises due to the presence of false alarms, but also to the presence of this new target. Such an issue can be overcome by using the Cheap JPDAF (Cheap Joint PDAF), which is indeed more suitable for a multi-tracking scenario.

However, Cheap (J)PDAF are not as reliable as the standard versions of these algorithms, as explained in par. 2.5.1.1.

The possible developments of the activity carried out during the three-year period, along with a wide campaign of validation of data acquired from real systems, may include further study of these algorithms.

In particular, the complete version of PDAF, therefore taking into account all the measures present in the validation area with a weight in estimating the target depending upon the likelihood of association of these measures with the target of interest, can be a useful tool to treat this kind of problems.

Similarly, in scenarios where many targets are present, it may be interesting to use the "M of N" (with M <= N) technique for the estimation of the state of the target, that is, the tracking of a target starts only if this it is present at least M times consecutively on N instants of time in the scene of observation or it may be declared "lost" if it is not present for at least M times.

Moreover, it would be useful to examine these and other algorithms on target no more point shaped, but "extended", in order monitor the movement of the cloud of points representing exactly the size of the two-dimensional target.

References

[1] J. Briggs, *"Target Detection by Marine Radar"*, The Institution of Electrical Engineer, 2004

[2] S. Kay, *"Fundamentals of Statistical Signal Processing"*, Volume II: Detection Theory. II, 1993

[3] V. Comincioli, "*Analisi numerica"*, ed Mc-Graw Hill.

[4] E. Brookner, *"Tracking and Kalman Filtering made easy"*, John Wiley & Sons, 1998

[5] D. Simon, *"Optimal state estimation"*, John Wiley & Sons, 2006

[6] M. Skolnik, *"Introduction to Radar Systems"*-3rd Ed. McGraw-Hill, 2002

[7] K. D. Ward, R. J., *"Sea Clutter: Scattering the K-Distribution and Radar Performance"*. IET Radar, Sonar and Navigation Series 20, 2006

[8] S. Watts, *"Radar detection prediction in sea clutter using the compound K-distribution model"*, IEEE Proceedings-F, vol.132(no.7), pp.613-620, 1985

[9] Y. Bar-Shalom and X. R. Li, *"Multitarget-Multisensor Tracking: Principles and Techniques"*, YBS Publishing, 1995

[10] Y. Bar-Shalom, X. R. Li and T. Kirubarajan, *"Estimation with Applications to Tracking and Navigation: Theory, Algorithms and Software"*, New York: Wiley, 2001

[11] Greg Welch, G. B. , *"An Introduction to the Kalman Filter"*, 1997

[12] Y. Bar-Shalom, (s.d.). *Recursive tracking algorithms: from the Kalman filter to intelligent trackers for cluttered environment*. pp 1-6.

[13] X. Rong Li, V. P., *"A Survey of Maneuvering Target Tracking: Dynamic Models"*, 2000

[14] X. Rong Li, *"The pdf of Nearest Neighbor Measurement and a Probabilistic Nearest Neighbor Filter for tracking in clutter"*. Proceedings of the 32nd IEEE Conference on Decision and Control, 918-923, 1993

[15]X. Rong Li, Y. B.-S., *"Theoretical Analysis and Performance Prediction of Tracking in Clutter with Strongest Neighbor Filters"*. Proceedings of the 1994 SPIE Conference on Signal and Data Processing of Small Targets, 2235, 429-440, 1994

[16]X. Rong Li, Y. B.-S., *"Tracking in Clutter With Nearest Neighbor Filters: Analysis and Performance"*. IEEE Transactions on Aerospace and Electronic Systems, 32(3), 1996

[17]Y. Bar-Shalom and E. T., *"Tracking in a cluttered environment with probabilistic data association"*, Automatica, pp.451-460, 1975

[18]Y. Bar-Shalom and J. A., *"Adaptive nonlinear filtering for tracking with measurements of uncertain origin"*, IEEE Conference on Decision and Control, pp. 243-247, 1972

[19]S. S. Blackman, *"Multiple Hypothesis Tracking For Multiple Target Tracking"*, IEEE A&E Systems Magazine, 19(1), 2004

[20]Y. Bar-Shalom, F. Daum and J. Huang, *"The Probabilistic Data Association Filter: Estimation in the presence of measurement origin uncertainty"*, IEEE Control Systems Magazine, 2009

[21]D. B. Reid, *"An algorithm for tracking multiple targets"*, IEEE Trans. Automat. Contr., vol. AC-24, no. 6, pp. 843–854, 1979

[22]Fortmann, T. E., Bar-Shalom, Y., and Scheffe, M., *"Sonar tracking of multiple targets using joint probabilistic data association"* ,IEEE Journal of Oceanic Engineering, 8, 3 (July 1983),173—183,1983

[23]K. C. Chang. *"Joint probabilistic data association for multitarget tracking with possibly unresolved measurements"* M.S.-thesis. Dep. Elec. Eng. Comput. Sci., Univ. Connecticut, Storrs. Sept . 198

[24]T. Fortmann, Y. Bar-Shalom, and M. Scheffe. *"Multi-target tracking using joint probabilistic data association"* in Proc. 19th IEEE Conf. Decision Contr.. Albuquerque. NM, Dec. 1980; and IEEE J.Ocean Eng. july 1983.

[25]R. J. Fitzgerald, *"Development of practical PDA logic for multitarget tracking by microprocessor"*, in Multitarget-Multisensor Tracking: Advanced Applications, Y. Bar-Shalom, Ed. Reading, MA: Artech House, 1990. pp: 1–23.

[26]Yao Liu ; Wei Zhang ; Mingyan Chen, *"Near Neighbor Cheap JPDA IMM based on amplitude information"*, Microwave and Millimeter Wave Circuits and System Technology (MMWCST), 2012 International Workshop , 2012 , 1-4

[27]Colegrove, S.B., Davey, S.J., Defence Sci. & Technol. Organ., Salisbury, SA, Australia, *"On using nearest neighbours with the probabilistic data association filter"*, Radar Conference, 2000. The Record of the IEEE 2000 International, 53-58.

[28]Kosuge, Y., Matsuzaki, T., Inf. Technol. R&D Center, Mitsubishi Electr., Kanagawa, Japan, *"The optimum gate shape and threshold for target tracking"*, SICE 2003 Annual Conference , 2152 - 2157 Vol.2

[29]Roecker, J.A., Phillis, G.L., IBM Corp., Boulder, CO, USA, *"Suboptimal joint probabilistic data association"*, Aerospace and Electronic Systems, IEEE Transactions on (Volume:29, Issue: 2), 510 - 517

[30]Ludeno, G. ; Brandini, C. ; Lugni, C. ; Arturi, D. ; Natale, A. ; Soldovieri, F. ; Gozzini, B. ; Serafino, F., *"Remocean System for the Detection of the Reflected Waves from the Costa Concordia Ship Wreck"*, Selected Topics in Applied Earth Observations and Remote Sensing, IEEE Journal of, July 2014, Volume 7, Number 7, ISSN 1939-1404, doi: 10.1109/JSTARS.2014.2321048

[31]B. C. Armstrong, H. D. Griffith, 'CFAR detection of fluctuating targets in spatially correlated K-distributed clutter', *IEE Proceedings-F*, vol.138, no.2, pp.139-152, April 1991.

[32]D. A. Shnidman, 'Radar detection probabilities and their calculation', *IEEE Transactions on Aerospace and Electronic Systems*, vol.31, no.3, pp.928-950, July 1995.

[33]P. Swerling, 'Radar probability of detection for some additional fluctuating target cases', *IEEE Transactions on Aerospace and Electronic Systems*, vol.33, no.2, pp.698-709, April 1997.

[34]D. A. Shnidman, 'Expanded Swerling target models', *IEEE Transactions on Aerospace and Electronic Systems*, vol.39, no.3, pp.1059-1069, July 2003.

[35]K. D. Ward, R. J. A. Tough, S. Watts, *Sea Clutter: Scattering the K-Distribution and Radar Performance*, IET Radar, Sonar and Navigation Series 20, (2006).

[36]K. D. Ward, 'Compound representation of high resolution sea clutter', *Electronics Letters*, vol.17, no.16, pp. 561-563, August 1981.

[37]D. J. Lewinski, 'Nonstationary probabilistic target and clutter scattering models', *IEEE Transactions on Antennas and Propagation*, vol.31, no.3, pp.490-498, May 1983.

[38]S. Watts, C. J. Baker, K. D. 'Ward, Maritime surveillance radar. II. Detection performance prediction in sea clutter', *IEE Proceedings-F*, vol.137, no.2, pp.63-72, April 1990.

[39]S. Watts, 'Radar detection prediction in sea clutter using the compound K-distribution model', *IEE Proceedings-F*, vol.132, no.7, pp.613-620, December 1985.

[40]S. Watts, K. D. Ward, 'Spatial correlation in K-distributed sea clutter', *IEE Proceedings-F*, vol.134, no.6, pp.526-532, October 1987.

[41]K. D. Ward, R. J. A. Tough, S. Watts, 'The physics and modelling of discrete spikes in radar sea clutter', in *Proceedings of the IEEE International Radar Conference 2005*, pp.72-77, 2005.

[42]S. Watts, K. D. Ward, 'Use of sea clutter models in radar design and development', *IET Radar, Sonar & Navigation*, vol.4, no.2, pp.146-157, 2010.

[43]E. Conte, M. Longo, 'Characterisation of radar clutter as a spherically invariant random process', *IEE Proceedings-F*, vol.134, no.2, pp.191-197, October 1987.

[44]E. Conte, M. Longo, M. Lops, 'Modeling and simulation of non Rayleigh radar clutter', *IEE Proceedings-F*, vol.138, no.2, pp.121-130, April 1991.

[45]A. Farina, F. Gini, M. V. Greco, L. Verrazzani, 'High resolution sea clutter data: statistical analysis of recorded live data', *IEE Proceedings on Radar, Sonar & Navigation*, vol.144, no.3, pp.121-130, June 1997.

[46]F. Gini, M. V. Greco, M. Rangaswamy, 'Statistical analysis of measured polarimetric clutter data at different range resolutions', *IEE Proceedings on Radar, Sonar & Navigation*, vol.153, no.3, pp.473-481, December 2006.

[47]S. Watts, 'Radar detection prediction in K-distributed sea clutter and thermal noise', *IEEE Transactions on Aerospace and Electronic Systems*, vol.23, no.1, pp.40-45, January 1987.

[48]Ludeno, G. ; Brandini, C. ; Lugni, C. ; Arturi, D. ; Natale, A. ; Soldovieri, F. ; Gozzini, B. ; Serafino, F., *"Remocean System for the Detection of the Reflected Waves from the Costa Concordia Ship Wreck"*, Selected Topics in Applied Earth Observations and Remote Sensing, IEEE Journal of, July 2014, Volume 7, Number 7, ISSN 1939-1404, doi: 10.1109/JSTARS.2014.2321048

[49]F. Serafino, G. Ludeno, C.Lugni, S. Flampouris, A.Natale, D.Arturi, F. Soldovieri *"Generation of bathymetric maps with high resolution through the analysis of Nautical X-Band Radar images"*, International Geoscience and Remote Sensing Symposium (IGARSS13), Melbourne (Australia), 22-26 July 2013

[50]G. Ludeno ,C. Lugni ,C. Brandini, A. Natale, D. Arturi, F. Soldovieri, F. Serafino, *"Diffracted Waves From the Aground Costa Concordia Cruise and Detected by the Remocean System"*, International Geoscience and Remote Sensing Symposium (IGARSS13), Melbourne (Australia), 22-26 July 2013

[51]F. Serafino, G. Ludeno, D. Arturi, C. Lugni, A. Natale, F. Soldovieri *"REMOCEAN: A marine radar as a safety tool for offshore platforms"*, European Geosciences Union (EGU2013), Vienna, 8-12 April 2013

[52]Gozzini, Bernardo; Serafino, Francesco; Lugni, Claudio; Antonini, Andrea; Costanza, Letizia; Orlandi, Andrea; Arturi, Daniele; Ludeno, Giovanni; Natale, Antonio; Soldovieri, Francesco; Ortolani, Alberto; Brandini,Carlo, *"An integrated sea monitoring systembased on a X-band wave radar to support the removal*

activities of the Costa Concordia wreck", EGU General Assembly 2013, held 7-12 April, 2013 in Vienna, Austria, p.12981

[53]Arturi, D. ; Serafino, F. ; Crocco, L., *"X band radar target tracking in Marine Environment: comparison of different algorithms in a real scenario."* EUCAP 10-15 April 2016 in Davos, Switzerland

Publications

Journal papers

[1] Serafino, F.; Lugni, C.; Ludeno, G.; Arturi, D.; Uttieri, M.; Buonocore, B.; Zambianchi, E.; Budillon, G.; Soldovieri, F.; *"REMOCEAN: A Flexible X-Band Radar System for Sea-State Monitoring and Surface Current Estimation"*, Geoscience and Remote Sensing Letters, IEEE , doi: 10.1109/LGRS.2011.2182031, 2012

[2] Ludeno, G. ; Brandini, C. ; Lugni, C. ; Arturi, D. ; Natale, A. ; Soldovieri, F. ; Gozzini, B. ; Serafino, F., *"Remocean System for the Detection of the Reflected Waves from the Costa Concordia Ship Wreck"*, Selected Topics in Applied Earth Observations and Remote Sensing, IEEE Journal of, July 2014, Volume 7, Number 7, ISSN 1939-1404, doi: 10.1109/JSTARS.2014.2321048

International conference proceedings

[1] F. Serafino, G. Ludeno, C.Lugni, S. Flampouris, A.Natale, D.Arturi, F. Soldovieri *"Generation of bathymetric maps with high resolution through the analysis of Nautical X-Band Radar images"*, International Geoscience and Remote Sensing Symposium (IGARSS13), Melbourne (Australia), 22-26 July 2013

[2] G. Ludeno ,C. Lugni ,C. Brandini, A. Natale, D. Arturi, F. Soldovieri, F. Serafino, *"Diffracted Waves From the Aground Costa Concordia Cruise and Detected by the Remocean System"*, International Geoscience and Remote Sensing Symposium (IGARSS13), Melbourne (Australia), 22-26 July 2013

[3] F. Serafino, G. Ludeno, D. Arturi, C. Lugni, A. Natale, F. Soldovieri *"REMOCEAN: A marine radar as a safety tool for offshore platforms"*, European Geosciences Union (EGU2013), Vienna, 8-12 April 2013

[4] Gozzini, Bernardo; Serafino, Francesco; Lugni, Claudio; Antonini, Andrea; Costanza, Letizia; Orlandi, Andrea; Arturi, Daniele; Ludeno, Giovanni; Natale, Antonio; Soldovieri, Francesco; Ortolani, Alberto; Brandini,Carlo, *"An integrated sea monitoring systembased on a X-band wave radar to support the removal activities of the Costa Concordia wreck"*, EGU General Assembly 2013, held 7-12 April, 2013 in Vienna, Austria, p.12981

[5] Arturi, D. ; Serafino, F. ; Crocco, L., *"X band radar target tracking in Marine Environment: comparison of different algorithms in a real scenario."* EUCAP 10-15 April 2016 in Davos, Switzerland